



北京航空航天大学
BEIHANG UNIVERSITY

2018 Undergraduate Team Aircraft Design

“Skylark” Hybrid-Electric General Aviation Aircraft



Presented by Beihang University, China

Aeronautical science and engineering school

Aircraft Design 2017-2018



Team member	AIAA numbers	signature
Chufan Guo	922534	郭楚凡
Zhuo Wang	922543	王卓
Ke Xu	922536	许珂
Ruichen He	920905	何睿辰
Kunyu Zhu	922539	朱坤宇
Xiaotian Gao	922562	高小天
De Huo	922540	霍德
Jinhan Wang	922649	王金瀚
Bo Li	922586	李博
Xiaoyue Zhang	922593	张晓岳

Advisor Chi Zhang

Chen Huang

Content

1. demand analysis	7
2. Global development	10
2.1 <i>Global Market Development Trends of General Aircraft</i>	<i>10</i>
1.1.1 Battery: Energy storage effect.....	10
2.1.2 Propulsion System: Efficiency and Weight.....	10
2.1.3 Pneumatic layout: Rectification/Wing body fusion	11
2.1.4 Sociality	12
2.1.5 Safety	12
2.1.6 Noise Reduction.....	12
2.1.7 Others.....	13
2.2 <i>Parameters for general aviation airplane.....</i>	<i>13</i>
3. Program design ideas.....	13
3.1 <i>Design requirements</i>	<i>14</i>
3.2 <i>Fuselage pneumatic layout selection</i>	<i>15</i>
3.3 <i>Wing position selection</i>	<i>15</i>
3.4 <i>Tail selection</i>	<i>16</i>
3.5 <i>Aircraft final layout.....</i>	<i>16</i>
4. Overall scenario Description.....	17

4.1	<i>Parameter tradeoffs</i>	17
4.1.1	Three major overall parameter (single parameter) tradeoffs	17
4.1.2	Parameter selection matrix & Matrix Curve	18
4.2	<i>Aircraft parameters</i>	20
4.2.1	Fuselage parameters	20
4.2.2	Wing parameters:	21
4.2.3	Tail parameters:	22
4.3	<i>The overall scheme and the trigram</i>	23
4.4	<i>Wing</i>	23
4.4.1	Material selection for wings.....	23
4.4.2	The material selection of the airfoil box	24
4.4.3	Airfoil position selection.....	24
4.4.4	Airfoil selection.....	24
4.4.5	Wing structure.....	25
4.4.6	The design of electric heating and deicing protection system for composite wing.....	27
4.5	<i>Tail</i>	28
4.5.1	Geometrical Parameters	28
4.5.2	Tail Area	29
4.5.3	Material and Weight.....	29
4.5.4	Rudders and Elevators.....	30
4.5.5	Airfoil.....	30

4.5.6	CATIA	31
4.6	<i>Fuselage</i>	31
4.6.1	The fuselage structure layout design.....	32
4.7	<i>Landing Gear</i>	34
4.8	<i>Main cabin</i>	34
4.9	<i>Power System Design</i>	35
4.9.1	Selection of engine and electric motor	35
4.9.2	Calculation of fuel consumption	39
4.9.3	Hydrogen mass estimation	39
4.9.4	Final choice of fuel cell.....	40
4.9.5	Reason and weight of lithium battery.....	40
4.9.6	Power Transmission System Design and Selection.....	41
4.9.7	Propeller selection and parameter display	42
4.9.8	Engine failure flight distance calculation.....	44
4.10	<i>Advanced Technology</i>	45
4.10.1	<i>Whole Parachute</i>	45
4.10.2	<i>anti-ice system</i>	46
4.10.3	Panorama Skylight	48
4.11	<i>general arrangement</i>	49
4.12	<i>weight analysis</i>	49

4.12.1	Approximate classification Gravimetric method.....	50
4.12.2	Statistical classification Gravimetric Method--comparison of four or six different algorithms.....	50
5.	Primary Performance analysis.....	51
5.1	<i>Engineering estimates for aerodynamic characteristics</i>	<i>51</i>
5.1.1	Clean Configuration Lift characteristics	52
5.1.2	Full machine lift characteristics	54
5.1.3	Take-off and Landing configuration	55
5.1.4	Resistance characteristics of clean configuration.....	56
5.1.5	Landing configuration resistance characteristics.....	60
5.2	<i>Flight Performance calculation</i>	<i>63</i>
5.2.1	flight envelope and ceiling calculation.....	63
5.2.2	Climb Performance	64
5.2.3	Voyage and Airtime	66
5.2.4	Take-off and landing performance calculation.....	67
5.3	<i>stability analysis.....</i>	<i>69</i>
5.3.1	Static stability analysis.....	69
5.3.2	dynamic stability analysis	70
6.	Analysis of competitive advantage.....	71
6.1	<i>Economic analysis.....</i>	<i>71</i>
6.1.1	Cost and usage costs.....	71

6.1.2	Comparison of the economic performance of the same type of aircraft.....	71
6.2	<i>Environmental protection analysis</i>	72
6.2.1	Carbon emissions analysis	72
6.3	<i>Competitive Advantage</i>	73
	Reference	75

List of figures

P.1.1	development trend of battery energy density	9
p.3.2.1	layout comparison.....	15
p.3.3.1	wing position comparison	15
p.3.4.1	tail comparison.....	16
p.3.5.1	aircraft layout.....	16
p.4.3.1	trigram of four-seats and six-seats aircraft.....	23
p.4.4.1	wing plan view size.....	23
p.4.4.2	wing structure.....	23
p.4.4.3	profil calculation result	25
p.4.4.4	wing inner structure	25
p.4.4.5	wing'panel connection structure	27
p.4.5.1	tail plan view size.....	30
p.4.5.2	tail space model.....	31
p.3.6.1	fuselage three-view drawing	31
P.3.6.4	Four-seats and six-seats fuselage	32

p.3.6.6 The main bearing structure.....	33
p.4.8.1 cabin plan view size	35
p.4.9.1 hybrid power transmission system	41
p.4.9.2 propeller and engine system.....	41
p.4.10.1 different states of parachute	46
p.4.11.1 four-seats six-seats aircraft inner structure.....	49
p.5.3.1 Pitch moment variation curve with angle of attack	69
p.5.3.2 Stability analysis of root distribution	70
p.5.3.3 Curve of longitudinal stability	71

1. demand analysis

1.1. design background

700 million tons -- that's the annual carbon dioxide emissions of the air transport industry. As global climate change intensifies, the industry is under pressure to change. In 2009, the general aviation manufacturers' association and the international business aviation committee worked together to reduce the environmental pollution of the general aviation industry. To be precise, these targets include a 2 per cent annual increase in fuel efficiency by 2020; zero carbon growth by 2020; And by 2050, carbon dioxide emissions will be cut by 50%. In February 2016, after six years of negotiations, 36 countries around the world, including China, finally agreed to the world's first commercial aircraft carbon reduction standard, and the new models introduced after 2020 must comply with this requirement. Under this pressure, many large companies are looking to the future, starting or accelerating investment in clean energy technologies.

In addition, in recent years, national regulators have become increasingly concerned about the growing problem of aviation noise. At large airports, the duration of general aviation flights continues to decline. The federal aviation administration (FAA) and the Canadian department of transportation (TC) are actively implementing stricter noise regulations. In the United States, the FAA has taken several steps, such as establishing the Noise Quest website and publishing several studies. In Canada, fines for noise related violations can be as high as 25,000 Canadian dollars (128,000 yuan). Under such pressure, general aviation aircraft manufacturers have to respond and want to produce quieter aircraft.

1.2. demand analysis

Aircraft development up to now there have been 100 years of history, from the beginning human desire to leave the ground, fly to the sky to now want to be more safe and reliable and energy saving advantage of convenient for people to live of flight, customer demand for aircraft has been a big change. Generally speaking, the following are the following:

1. Now purely rely on lithium battery, its properties, such as energy density increased by 50% to 100% at least in the existing situation, need to use a hybrid way of extended range, and improve the reliability of the energy in the flight.

2. Now the price of jet fuel is higher, in the context of current trends, the future of oil resources shortage even dried up when the price will be higher, need to try other energy as possible to promote the development of aircraft on the environmental protection.

When choosing energy, you also need to take into account the requirements of cost and service life.

3. Compared with the United States, China's general aviation is relatively deficient, and the aircraft needed to be designed can accommodate as many missions as possible and have as far as possible.

4. General aviation in China is in the social benefit at present (such as earthquake emergency rescue, etc.) to the design of aircraft can gradually develop its economic benefits, even can have similar to the development of tourism, and other good prospects.

5. If you consider the air travel industry development, needs further to passengers aboard environment such as vision, engine noise, normal flight stability, cabin interior space and beautiful shape on the whole plane put forward higher request to attract tourists, promote the development of the industry.

6. Now China's development of facilities, such as the airport is far from the United States so developed, need the aircraft designed to all kinds of the runway, and even more complex environment and terrain open land and take off.

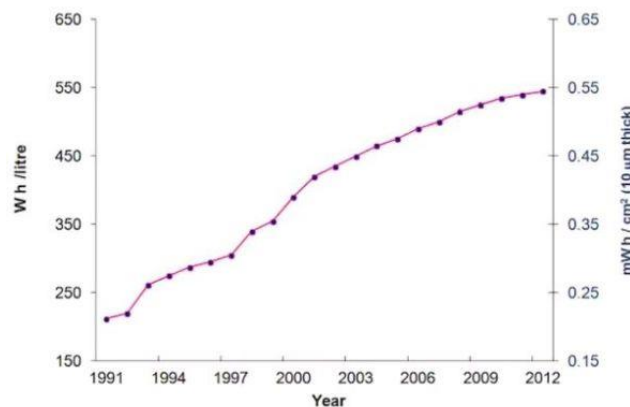
7. The airspace of China is now heavily restricted to the no-fly zone. Meanwhile, the number of professional technicians (especially pilots) in China is not enough, so it is necessary to have certain autonomous driving ability. At the same time, the aircraft also needs to be used as far as possible in less hostile environments, requiring the ability to receive signals from navigation devices to communicate.

8. If the price can be dropped to a certain extent, can be considered as a private jet to sell, the need for aircraft parking space, warranty maintenance, price cheap and convenience request parts replaced.

For the eight details above, here are two main points: energy dynamics and overall flight characteristics.

In terms of energy problem, this is a hybrid of general aviation aircraft design key points, not only need to consider the energy environmental protection problems, provide energy for power power, the requirement of flight distance, supplement energy convenience (charging, inflatable, refueling convenience, etc.) have great influence. At the same time, general aviation is also likely to be used in the case of disaster relief, which requires energy to maintain an altitude of more than 1800km at a speed of 300km/h. And in order to adapt to a variety of complex terrain, the engine needs energy to provide enough power to enable safe takeoff and landing on different roads.

Current lithium-ion batteries, such as tesla's 18650 battery, have an energy density of 250Wh/kg, but Wright Electric predicts that the energy density will be at least 50% to double to meet the requirements. As shown in the figure below, this is the development trend of battery energy density figure in recent years, apparently in accordance with the trend we need to look for other way such as fuel cells, with the use of lithium-ion batteries in order to maintain long high speed of the plane.



P. 1.1 development trend of battery energy density

The overall nature of the aircraft is primarily aerodynamic and structural. For aerodynamic layout, it involves the flight stability and control of the aircraft. For the aircraft used for the development of tourism, the passenger ride comfort has certain requirements; For disaster-relief aircraft, it may be used to transport critical patients, so it is not too bumpy to fly or even take off. For plane of general layout, the plane's engine position size will affect the noise of the passengers, the wing aspect ratio and the tail of the form and layout can affect the appearance of the plane, this will be the a factor of the development of air travel. At the same time, the overall layout will affect the lift-to-drag ratio of the aircraft, thus coupling with the energy dynamic, so this demand is not negligible.

Generally speaking, the specific requirements of the requirements:

1. The take-off weight is as small as possible;
2. Aircraft energy should be able to control system coordination to ensure sufficient power and environmental protection;
3. Try to reduce drag and increase, reduce the demand for energy and increase the voyage;
4. Choose international or national standard product spare parts to facilitate aircraft maintenance;
5. Control the ground Angle and take-off Angle, and adapt to various environmental surfaces;
6. On the basis of satisfying the previous points, design a beautiful appearance and add comfort level.

2. Global development

2.1 Global Market Development Trends of General Aircraft

1.1.1 Battery: Energy storage effect

The current mainstream technology alternative to petroleum is lithium batteries and fuel cells. The biggest advantage of fuel cells is their high energy density, which is 120 times that of lithium batteries. However, lithium batteries start early, commercialization is higher, the cost of the whole vehicle is lower, and the charging can use the existing power grid system. Compared to the entire network of fuel cell hydrogenation and hydrogen supply, it needs to be built from scratch. Also lower. Therefore, the core of competition between the two is energy density and cost competition. The cost reduction is an engineering problem that can be solved through commercialization. However, the energy density is facing bottlenecks in the basic science field. In the long term, fuel cells will undoubtedly have greater potential and are most likely to become the next generation of basic energy. (but need to consider how to reduce the cost of the fuel cell and improve its safety).

2.1.2 Propulsion System: Efficiency and Weight

(1) Motor efficiency:

At present, the average efficiency of small and medium-sized motors is 87%, and the international advanced level is 92%, but the proportion of high-efficiency and energy-saving motors is low. According to the sample survey of the application, the proportion

of high-efficiency and energy-saving motors that achieve Grade 2 or above is only 8%. This has caused a great waste of the entire social resources. Therefore, the application and promotion of high-efficiency motors must be one of the trends in the future.

(2) Matching efficiency of "mixed type":

The current combination of methods used more "parallel connection", that is, the fuel engine and battery motor drive the propeller through power deployment. Although this kind of layout method is light, it can not adapt well to the needs of various flight conditions. Therefore, "hybrid connection" came into being: at low speed, the hybrid connection is mainly operated in "series" (independent control) mode; at high speed, Hybrids are mainly operated in a "parallel connection" (joint work) mode; when taking off and landing, they can be directly driven by a motor. This combination method can ensure that the aircraft is in the most efficient and economical operation at all times, but it needs to identify and judge the flight status, power switch, and emergency disposal under emergency conditions, so as to ensure its highest economy. The development of this area is very large and has a good prospect. It has become one of the key development trends.

(3) Fusion weight of motor, battery and engine:

The "hybrid type" power combination referred to in (2) above has a large structure and complex mechanism. The weight and volume occupied by the motor, battery, and engine can be reduced by the effective fusion and structural optimization. The development of type combinations will become a difficult point to tackle.

At the same time, a new generation of electric turbofan engines is being studied (such as the revolutionary engine technology mentioned in the new concept machine of Zunum Aero). If the energy conversion efficiency can be further improved and some key technologies can be solved, General aviation may usher in a new technological revolution.

2.1.3 Pneumatic layout: Rectification/Wing body fusion

The junction between the fuselage and the trailing edge of the wing creates a dead-water zone. Rectifying this area or integrating the wing body can reduce flight resistance, increase lift, and allow more room for fuel or batteries. For example, NASA's x48 verifier is the exploration and research of the BWB (blended wing body) technology. In the future, through the application of

BWB, the aerodynamic performance of the aircraft can be effectively improved, and then the fuel consumption during the flight process can be reduced, making the flight more economical. This will also make the general aviation market, which is depressed after the economic crisis, usher in a recovery.

2.1.4 Sociality

Due to the economics of hybrid general aircraft, as the density of aviation networks increases, its social functions will gradually appear, such as: sightseeing tours, inspections, medical transportation, and emergency disposal. In addition, with the reduction of runway requirements for hybrid aircraft, it will be more suitable for emergency rescue and other incidents.

2.1.5 Safety

Although flight safety has been improved in recent years, and the number of fatal accidents has decreased year by year, there are still many flying accidents every year, most of which are due to the pilot losing control of the aircraft or exhausting the fuel of the aircraft. According to the report of the NTSB, about 50 airplanes each year lose their power crash due to the exhaustion of fuel or the failure of fuel supply to the engine. This accident, which could have been easily avoided, was not resolved because of the current technology. Therefore, how to further enhance the safety in the flight process is also one of the future development directions. With the gradual development of artificial intelligence in recent years and the continuous improvement of flight control algorithms, pilot manipulation by AI has gradually become one of the research directions. Perhaps in the near future, AI will completely replace people and achieve complete control of aircraft. This may solve the problem of the aircraft crashing due to fuel depletion during the flight.

2.1.6 Noise Reduction

Another major development of general aviation is the research on noise reduction. This is mainly done through research and improvement of the engine. Research experts in this field are trying to reduce the impact of noise generated by engine operation on the occupants of the aircraft by changing the structure of the engine, the materials used, and the location of the engine. The entire general aviation field is advancing toward the era of small noise.

2.1.7 Others

There are items such as "unmanned control (automatic take-off and landing)", "further use of carbon fiber (or new) composite materials (reducing costs, etc.)", "high-end internal configuration (application of panoramic windows)", "military small and medium-sized general purpose Platform (military patrol)" and so on.

2.2 Parameters for general aviation airplane

Graph	Name	Length(m)	Weight (kg)	Cruising speed (km/h)	Range (km)	Engine
	A500	11.43	3175	425	2850	TSIO-550E
	SR20	7.92	1383	259	1453	IO-360-ES
	SR22	7.9	1542	405	1850	IO-550-N
	SF50	9.42	2650	560	1942	FJ33-4A-19
	Comp Air11	11.6	3538	666.72	3704	TPE331-14GR
	Comp Air12	12.6		482	4080	TPE331-14GR
	Comp Air9	11.6	3492	408	2778	TPE331-10
	Comp Air10XL	9.45	2359.0	209	1472.00	Walter M601D

3. Program design ideas

3.1 Design requirements

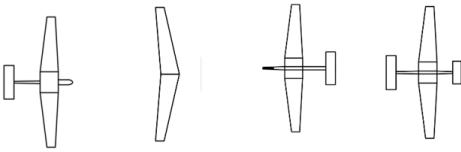
According to the requirements of the aircraft performance and the previous market demand analysis, we compare the performance of the same type of aircraft in the market, and re-integrate the design concept of Skylark to get the final basic design index requirements.

Project requirements	Our design
Ability to visually fly and fly through autopilot	The man-machine environment analysis shows that the visual angle is good and an automatic driving system is installed at the same time.
Ability to fly under known icing conditions	Use TKC ice protection system
Use engine that will serve in 2028	Lycoming AEIO-360-A four-cylinder piston engine
Use the motor that will be put into use in 2028	New Siemens motor not sold
Battery energy density	350Wh/kg
Battery power density	3.1kW/L, 2.0kW/kg
Motor efficiency	95%
Propeller efficiency	90.473 when cruising, 0 when taking off
Electric propulsion system weight	125kg
4-seat and 6-seat universal body structure and push weight system weighs at least 75%	Satisfy the conditions, the weight of the four or six seats is exactly the same, and the weight of the body structure is almost the same
The maximum distance that a battery can reach when a single failure occurs	Four seats 960km

Project requirements	unit	Our design	
		4 seats	6 seats
Flight 1852/1389	km	2005	1503
Cruising speed 392/465	km/h	392.8	466.5
Climb rate 8.0 / 7.0	m/s	8.58	7.97
Takeoff Distance - Concrete Place 457/548	m	345.8	432.7
Departure distance - Meadow 420/550	m	359	401
Landing distance - concrete 547/548	m	422.36	513.27
Landing Distance-Grass 420/550	m	422.36	513.27
Maximum stall speed 80/80	km/h	149	162
The maximum flying speed 430/410	km/h	456.5	453.6
Payload 400/600	kg	419	602

3.2 Fuselage pneumatic layout selection

Aircraft aerodynamic layout tradeoffs.




Performance	Performance Weight	Each layout weight			
		General layout	Flying wing layout	Duck layout	Three wing layout
Lightweight	3	2	5	3	2
Large lift	2	3	2	5	4
Small resistance	1	1	5	4	3
High stability	5	5	1	3	5
High reliability	5	5	1	2	3
Simple to manufacture	2	5	1	3	3
Total weight	18	73	36	54	63

p. 3.2.1 layout comparison

Considering that the hybrid aircraft needs to carry two kinds of energy engines, we put forward these requirements for the fuselage layout on the left side of the table, and after weighing and comparison we chose the general layout with the highest total weight score.

3.3 Wing position selection

Wing position tradeoffs.



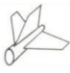



Performance	Performance Weights	Upper wing	Single wing	Lower wing
Lightweight	3	5	3	5
Good stability	5	4	3	2
Low noise	4	1	3	5
Simple to manufacture	2	4	1	5
Total weight	14	47	38	55

p. 3.3.1 wing position comparison

Although the stability of the lower single wing is not as above as that of the single wing, the main purpose of the design of this hybrid electric aircraft is to protect the environment, so the noise and the weight of the empty aircraft can not be ignored either. In addition, as a general-purpose aircraft, passenger comfort and sightseeing functions are also the focus of our development.

3.4 Tail selection

According to the actual situation, the weights of different types of tails are listed, and the weight of the double-tailed support itself is heavy, but it can effectively reduce the weight of the whole machine and increase the lift. However, the Take-off and landing performance is not as good as that of other structures.

Tail balance					
Performance	Weight	Conventional tail	T tail	V tail	Twin tail support
Lightweight	3	3	2	4	2
Small resistance	1	3	3	5	2
Stability and manoeuvrability	4	3	5	2	4
High reliability	4	4	4	3	4
Simple to manufacture	2	5	4	5	2
Total weight	14	50	53	47	44

p. 3.4.1 tail comparison

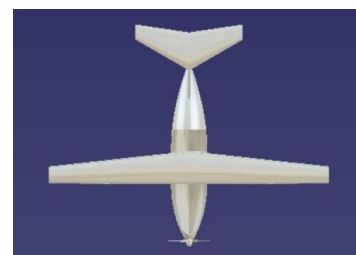
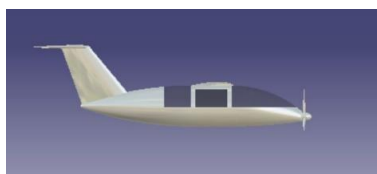
Therefore, we gave up the plan for the twin-tailed aircraft and selected the T-tail with a high weighted score.

3.5 Aircraft final layout

The aircraft adopts high mounted wing, T-tail layout with single engine.

Advantages: the high mounted wing increased roll stability, while inverted dihedral increased stability as well. The use of T-tail can reduce the flat tail area.

Disadvantages: Large resistance. The wings influence the air flow through the tail, causing it easy to stall.



p. 3.5.1 aircraft layout

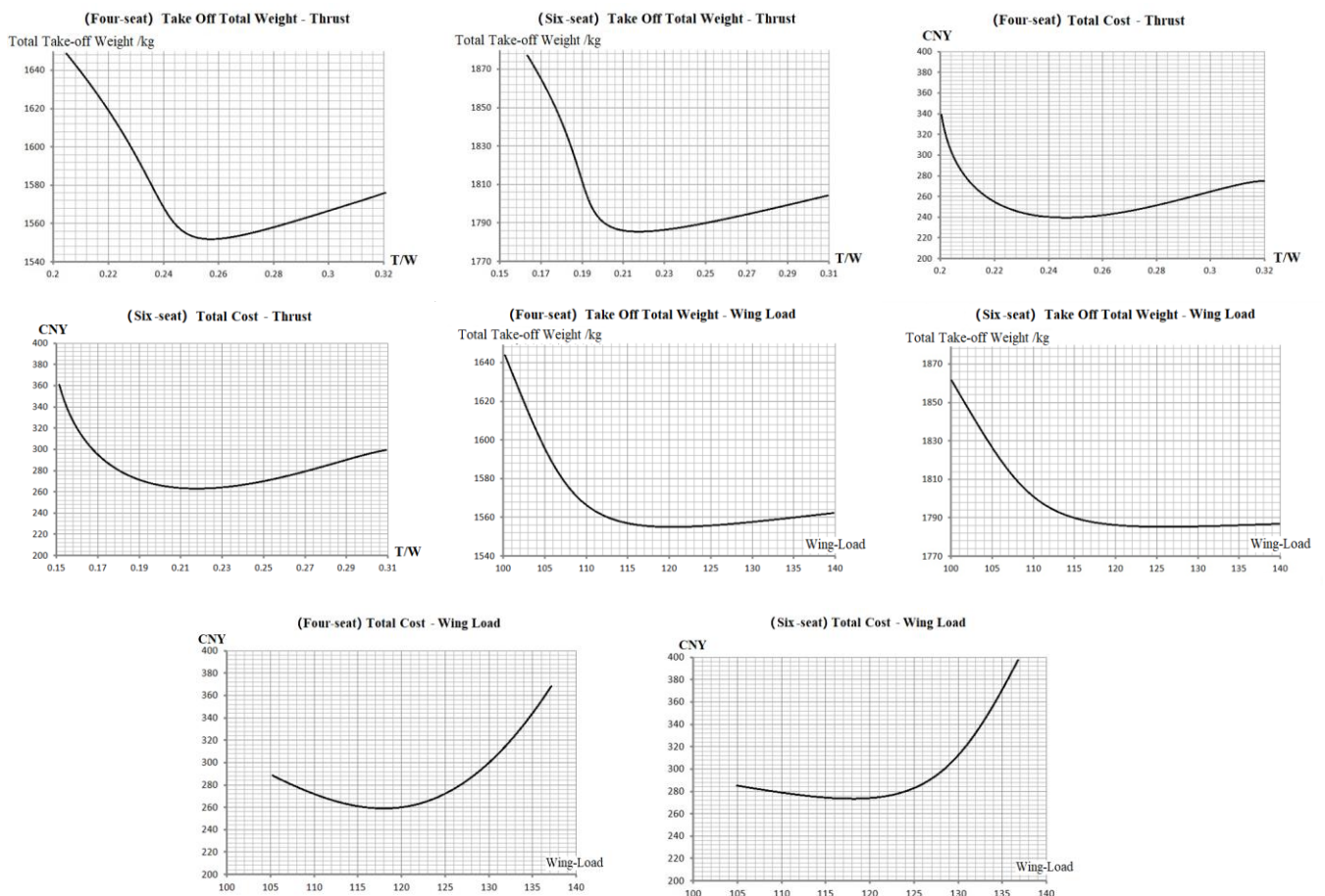
4. Overall scenario Description

4.1 Parameter tradeoffs

4.1.1 Three major overall parameter (single parameter) tradeoffs

(1) Push-to-weight ratio & wing load trade-off

The overall parameter tradeoffs include three categories: design parameter tradeoffs, demand trade-offs and growth sensitivity trade-offs. Among them, the first category of design parameter trade-offs is the trade-off between push-to-weight ratio T/W and wing load W/S. The following is the relationship between the six total take-off weight and thrust-to-weight ratio and the relationship between the four-six-seat cost and thrust-to-weight ratio and the relationship between four-six-seat total take-off weight and the wing load and the relationship between four and six seats and the wing load.



According to the four-or-six-seat "Take off total weight-wing load" tradeoff chart and "cost-wing load" tradeoff chart, after weighing the value of the wing load: 114.68kg/m² for four seat, 119.41 kg/m² for six seat. According to the four or six-seat "Take

off total weight-thrust" tradeoff and "cost-thrust ratio" tradeoff, after weighing the thrust than the value of: 0.248 for four seat, 0.207 for six seat.

(2) Other typical parameter tradeoffs

Similar to the first part of the "thrust" and "wing load" weighing methods, combined with a certain reference and light general aviation aircraft examples, can give the following three tables: Design Parameters Weighing Table, Demand Balance Table, Growth Sensitivity Balance Table.

The main constraints of the design parameters are: To meet the given set of mission and performance requirements, as far as possible to reduce the weight and cost of aircraft, so according to the design requirements for each of its single parameters and Take-off total weight and cost balance.

	Four-Seat	Six-Seat		Four-Seat	Six-Seat
T/W	0.248	0.207	Tail Wing	T	T
W/S	114.68kg/m ²	119.41kg/m ²	Number of Engines	1	1
Aspect ratio	10.8	10.8	Engine Form	Piston engine	Piston engine
Lead Sweep Angle	2°	2°	Passengers	2+2	2+2+2
Taper Ratio	0.5	0.5	Advanced Technology	Panoramic Skylight	
Airfoil Relative Thickness	11%	11%		The Whole Parachute	

The main constraints to the demand trade-off are: first of all, the sensitivity of the change of aircraft weight or cost caused by the change of design requirements is determined, and the design requirements for some forced weight and cost increase are relaxed, so the slope of the total take-off weight and the curve of the cost with single parameter should be considered. The steeper the curve, the more careful it is to weigh the selection of parameters. The main constraint of the growth sensitivity tradeoff is: By analyzing the influence of the percentage of the change in the design parameters on the weight percentage, the influence of the relative parameters on the aircraft weight and cost is determined, and the relevant parameters are selected.

	Four-Seat	Six-Seat		Four-Seat	Six-Seat		Four-Seat	Six-Seat		Four-Seat	Six-Seat
Voyage	1900	1400	Maximum overload	2.8	2.8	Structure Weight/kg	547.03	642.47	Trust	388.45	388.45
Payload /kg	400	600	Runway Length	457.2	548.64	Zero-lift Resistance Coefficient	0.017	0.017	Unit Fuel Consumption	0.1437	0.1437
Passengers	1+3	1+5	Acceleration Time	20	23	Maximum Lift-drag Ratio	17	17	Fuel Price	3.593¥/kg	
Await time /min	30	30	Climb Time/min	8.5	9.5	Maximum Lift Coefficient	1.21	1.21			
Speed /km/h	325/380/430	325/380/430	Cost	260w	280w						

4.1.2 Parameter selection matrix & Matrix Curve

(1)The relationship between take-off weight and thrust ratio and wing load .

The relationship between thrust ratio and wing load can be expressed as: $W_0=f(T_0/W_0, W_0/S)$, and in the previous Take-off weight formula does not take into account the impact of thrust ratio, wing load on Take-off total weight, it is necessary to estimate the formula (mainly for each stage weight ratio) to be revised, see: Raymer D.P. Modern aircraft design[M].Zhongdingkui.Beijing: National Defense Industry Press, 1992

Then through the compiled iterative program can be achieved: input specified thrust than t/w and wing load w/s , can be iterated to get a new round of take-off total weight.

2)Parameter selection matrix and parameter selection matrix superimposed on constraint curve .

These performance parameters are weighed in a similar way to the take-off weight, so only the weighing process of take-off weight, the results, and the tradeoff of take-off and landing distances, landings and sea level climb are given below: thrust is about 20% more than t/w .

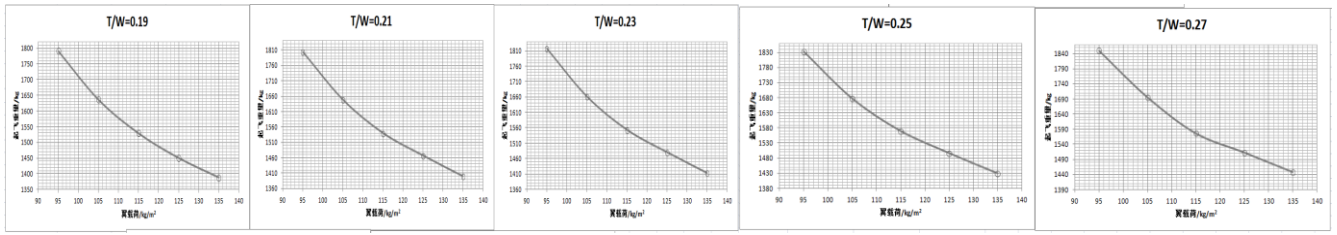
Amplitude change: From 0.23 to both sides to take four values, interval 0.02, the following figure:

	T/W				W/S (kg/m ²)					
	0.19	0.21	0.23	0.25	0.27	95	105	115	125	135
W/S=95kg/m ²										
W/S=105kg/m ²										
W/S=115kg/m ²										
W/S=125kg/m ²										
W/S=135kg/m ²										
T/W=0.19	1791.38	1636.33	1528.78	1450.06	1387.88					
T/W=0.21	1803.85	1648.89	1540.45	1467.48	1400.01					
T/W=0.23	1817.58	1662.12	1554.36	1481.56	1414.36					
T/W=0.25	1832.65	1677.25	1569.64	1496.68	1429.45					
T/W=0.27	1850.35	1695.68	1576.25	1512.85	1447.98					

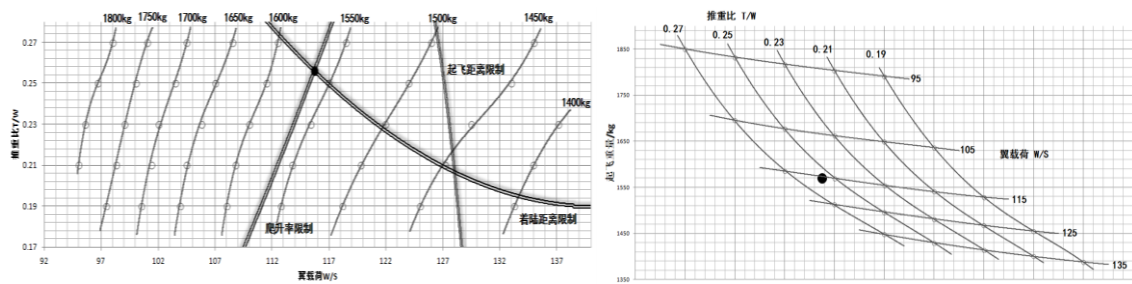
Wing load w/s for about 20% amplitude changes: Taking into account the first part of the curve trend, so from the 115kg/m² to the left of three values, to the right to take a value, the interval of kg/m², as shown above.

The combination of different thrust ratios and wing loads can get a new round of takeoff weight in the preceding iterative program, and fill in the table

According to the thrust ratio and the change of the wing load, the variation of the take-off weight with the wing load is drawn under different thrust conditions:



Then the parameter selection matrix curve and the parameter selection matrix curve with the performance constraint curve can be drawn. The three constraint curves are given according to the design requirements. At the same time, the blanket diagram can be made, and the constraint points obtained by the parametric matrix curve are marked on the graph.



According to the image can be weighed after the thrust than the $t/w=0.256$, wing load $w/s=115.72\text{kg/m}^2$, take-off total weight $w=1569.64\text{kg}$.

The above four-type parameters, the same can draw a six-seat curve, the six-seat balance after the thrust than $t/w=0.218$, wing load $w/s=120.09\text{kg/m}^2$, take-off total weight $w=1847.03\text{kg}$.

4.2 Aircraft parameters

4.2.1 Fuselage parameters

	Four-seats aircraft	Six-seats aircraft
Total length	7.75	9.25
Maximum equivalent diameter of section	1.71	1.71
The fuselage height	1.7	1.7
The length of the front of the fuselage	2.6	2.6
The middle length of the fuselage	1.5	3

Tail length	3.65	3.65
λ_{body}	4.53	5.41
λ_{head}	1.52	1.52
λ_{tail}	2.13	2.13

4.2.2 Wing parameters:

Wing relative area S	15.38 m ²
Wing span b	12.89 m
root chord Cr	1.641 m
tip chord Cl	0.746 m
mean aerodynamic chord	1.250 m
mean aerodynamic chord position	2.819m
Root-tip ratio	2.2
span-chord ratio A	10.8
Lead edge sweepback	2degree
Trailing edge sweepback	5.55 degree
1/4string sweepback	0.8 degree
Anhedral	6 degree
Root-tip ratio	2
established angle	2 degree
torsion angle	-3 degree
weight	184.1678kg

Wing flap:

Relative chord	20%=0.2386m
area	12%=1.8456m ²
span	2.45m

Ailerons:

Relative string	23%=0.27439m
area	12%=1.8456m ²
span	1.9m

4.2.3 Tail parameters:

Vertical tail parameters	value	Flat tail parameters	value
tail capacity	0.091	tail capacity	0.430
area (m^2)	2.71	area (m^2)	1.350
span (m)	2.088	span (m)	3.00
tip chord length (m)	0.836	tip chord length (m)	0.300
root chord length (m)	1.828	root chord length (m)	0.60
The distance from root string to fuselage axis (m)	0.30	The distance from root string to fuselage axis (m)	1.723
Lead edge sweepback ($^\circ$)	40	Lead edge sweepback ($^\circ$)	11.31
Trailing edge sweepback ($^\circ$)	70	Trailing edge sweepback ($^\circ$)	0
established angle ($^\circ$)	2	established angle ($^\circ$)	-1.2
torsion angle ($^\circ$)	0	torsion angle ($^\circ$)	0

The joint part of the SPAR and fuselage	constructional steel	7.85	0.0007	5.42
Leading edge	glass fiber reinforced plastics	1.5	0.002	3.5
Trailing edge	TiGr layer board	4.52	0.002	9.04
The wing wall	7075 aluminium alloy	2.1	0.059	123.9
Wing girder structure	7475-T7351 aluminium alloy	2.82	0.015	42.3

4.4.2 The material selection of the airfoil box

Wing box parts	Material type	material trademark	1.8
Upper skin	Carbon fiber prepreg	BAMS 532-027	1.8
Upper skinned trusses	Carbon fiber prepreg	BAMS 532-027	1.8
Lower skin	Carbon fiber prepreg	BAMS 532-027	1.8
Lower skinned trusses	Carbon fiber prepreg	BAMS 532-027	1.8
Beam	Carbon fiber prepreg	BAMS 532-027	1.8
Rib	Plank	aluminium alloy 7475	2.78

The use of advanced metal materials make it have a strong antifatigue, fireproofing, anti-destruction and corrosion resistance ability. The weight is reduced, thus greatly reducing fuel consumption and emission and reducing operation cost.

4.4.3 Airfoil position selection

The wing adopts the low-wing layout, which has a high structure strength. The wing runs through the fuselage, reducing the structure weight of the aircraft. It is beneficial to the strength and integrity of the glass fuselage and the low-wing plays a protective role on the fuselage in the emergency landing.

4.4.4 Airfoil selection

The wing adopts the NACA2411 airfoil, which has the most favorable pressure distribution near the design lift coefficient. The drag coefficient is the smallest and the lift drag ratio is relatively large.

$$W = 1/2 \rho v^2 * C_L * S$$

Design airfoil lift coefficient: $C_{L} = (W/S) = 1/q = 0.15$

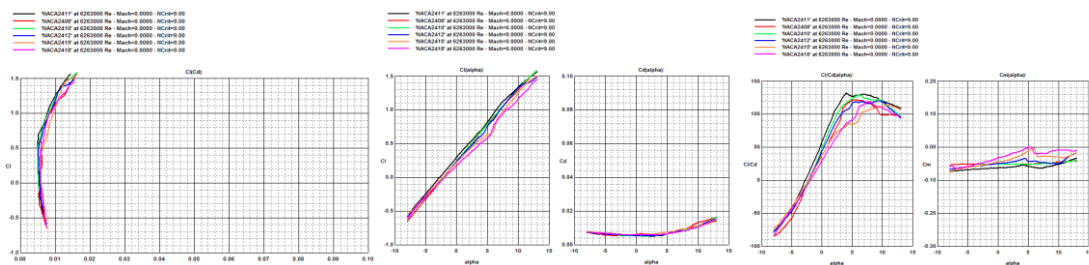
Plane airfoil lift coefficient: $C_l = 0.2$

It is considered that the lift coefficient of a three-dimensional wing = the lift coefficient of a two-dimensional wing.

NACA2411 lift angle coefficient is $C_l = 0.3$ when the attack angle is zero, which satisfies the lift coefficient requirement of the design airfoil.

In the vicinity of the design lift coefficient, NACA airfoil has the most favorable pressure distribution. Its resistance coefficient is the smallest. The lift drag ratio is large, and it has a better stall performance.

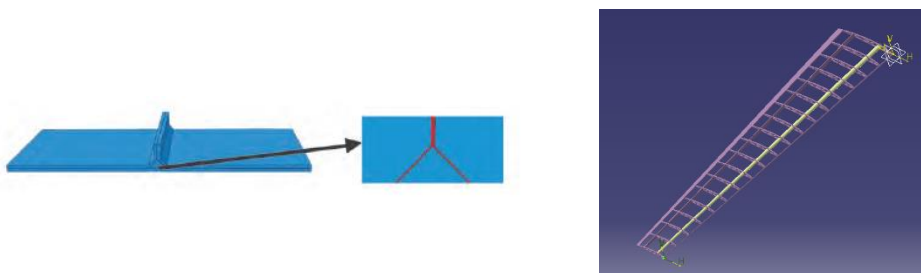
The five airfoil curves of the NACA24 series are shown below. For cruising speed $M = 0.32$, when lift coefficient is about 0.2-0.3, NACA2411 is more favorable, and airfoil resistance is minimum during cruising flight.



p. 4.4.3 profili calculation result

4.4.5 Wing structure

The wing adopts composite material integrated wall panel structure, which the inner structure adopts beam structure layout.



p. 4.4.4 wing inner structure

The low cover of the wing is provided with a cover for sealing, assembly and maintenance of the whole fuel tank. The inspection port should be placed in the place with less influence on the strength, so as not to damage the main bearing structure as far as possible.

The location of the inspection port can be cut off at the bottom of the lower panel along a long truss axis to minimize the stress on the lower panel. In order to meet the requirement of internal accessibility of the wing box, the center line of the maintenance center should be as close as possible to the chord middle position of the wing. Along the wing span, there should be a repair Bay between the two ribs except for places that has the structural constraints.

The inspection port is elliptical, and the long axis of the inspection port is located on the axis of the center long truss, which has basically the same distance from the front and rear beams. The wing height decreases gradually along the wingspan, and the reachability requirement gradually changes. The diameter of the maintenance mouth decreases from the wing root to the tip.

To meet airworthiness requirements and functional requirements, overhaul covers meet the following technical requirements.

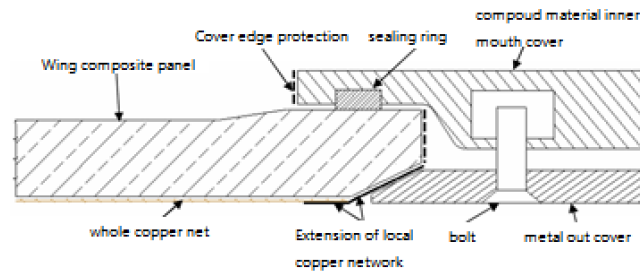
- (1) can be disassembled to meet the requirements of assembly and maintenance.
- (2) meet the seal requirements of the tank.
- (3) follow the aerodynamic shape of the lower panel.
- (4) protection requirements for impact damage of discrete source.
- (5) lightning protection requirements.
- (6) fire protection requirements and so on.

The clamp is used and the composite material is selected. The clamping cover is a nonbearing mouth cover, which is composed of an inner and an outer cover, and the inner and outer mouth covers are clamped on the skin by bolts. The gripper cover should consider the lightning protection between the skin and the cover. The clamping cover is easy to disassemble, which is beneficial to improve the maintenance performance of the aircraft and the sealing performance of the fuel tank. When the outer wing is bent, the gripper cover is not involved in the overall load transfer of the outer wing, and is suitable for the fatigue sensitive area, but the cap

itself bears the oil pressure load. The problem of electrochemical corrosion of aluminum alloy cover and contact compound skin is very serious, which is against the requirement of anticorrosion treatment and lightning protection for aluminum alloy mouth cover.

Therefore, the composite cover of the wing is preferred.

Design of the interface between the lid and the wall panel is as the picture followed:



p. 4.4.5 wing' panel connection structure

The lightning protection design of the gripper lid adds a metal mesh outside the outer lid to form an effective electrical path between the panel and the panel.

The cover of the compound wing box is sealed with groove. The grooves are arranged on the mouth cover to avoid grooves on the skin and reduce the possibility of damage to the composite skin.

4.4.6 The design of electric heating and deicing protection system for composite wing.

According to the switch signal on the control panel, the signal of the ice detection system and the temperature feedback signal of the heating element, the controller component controls the heating time and the heating power of the heating element, thus converting the electric energy into heat to prevent the ice from the wing front edge.

Advantage:

(1) High efficiency and low energy consumption. There is no loss of heat energy in the system pipeline. And the thermal efficiency can reach more than 75%, far higher than the 50% of hot gas anti icing. In addition, to achieve the same effect, the energy consumption of the electric heating / anti icing system is less than that of the 67%.

(2) The structure is simple, the maintenance and the reliability are high. The structure of pipeline, valve and ice protection chamber is eliminated, and the system structure is simplified. Besides, the setting and partition design of heating pad can greatly improve the maintenance and reliability of the system.

(3) Green and environmental protection. In spite of the slight increase in power supply, the exhaust emission can be reduced and the noise pollution of the engine can be reduced in general.

When the aircraft is cabled, the A and B channels are used to isolate the electrical line interconnection system (Electrical Wiring Interconnection System, EWIS), so as to meet the requirements of the channel isolation and the redundancy of the electrical lines.

4.5 Tail

4.5.1 Geometrical Parameters

Vertical Fin	Parameters	Horizontal Tail	Parameters
The tail capacity	0.091	The tail capacity	0.862
Area (m^2)	2.71	Area (m^2)	4.89
Span (m)	2.088	Span (m)	4.03
Tip chord (m)	0.836	Tip chord (m)	0.376
Root chord (m)	1.828	Root chord (m)	0.836
Distance between root chord and the axis of fuselage (m)	0.30	Distance between root chord and the axis of fuselage (m)	2.71
Forward sweep angle ($^\circ$)	40	Forward sweep angle ($^\circ$)	15
Backward sweep angle ($^\circ$)	69.88	Backward sweep angle ($^\circ$)	2.27

Roll angle (°)	0	Roll angle (°)	0
Setting angle (°)	2	Setting angle (°)	2
Twist angle (°)	-3	Twist angle (°)	-3
Taper ratio	0.46	Taper ratio	0.45
Mean aerodynamic chord length	1.394	Mean aerodynamic chord length	0.635
Tail arm	6.101	Tail arm	6.101
Weight (kg)	68.107	Weight (kg)	41.8726

4.5.2 Tail Area

The tail is designated as a T-tail and the weight is much heavier than the conventional one, so the tail must be strengthened to support the horizontal tail. The advantage is that since the end plate effect is present, the tail can be smaller, so the smaller is chosen. It is necessary to raise horizontal tail to avoid the wing wake and propeller slip stream, so that the efficiency can be increased to reduce the size of the tail. Therefore, the height of vertical fin is designed to be 2.088m. Also, due to the fully-active tail, the tail capacity factor can be reduced by 10%; due to the end plate effect, the vertical fin capacity is sparsely reduced by about 5%; and the horizontal tail capacity factor can be reduced by 5% due to the undisturbed airflow. The area of the vertical tail was effectively reduced, and horizontal tail was 2.454 m² and vertical fin is 2.71 m² at the area.

4.5.3 Material and Weight

The vertical wing center wing box structural material is mainly made of super-hard aluminum, supplemented by composite carbon fiber.

Using advanced metal materials, the wing has strong anti-fatigue and anti-corrosion capabilities as well as strong fire and vandal-proof capabilities. Reduced weight, which greatly reduces fuel consumption and emissions, and reduces operating costs.

Skin weight: Horizontal tail: 11.672kg Vertical tail: 15.406kg

Total:

Horizontal tail: 41.8726kg

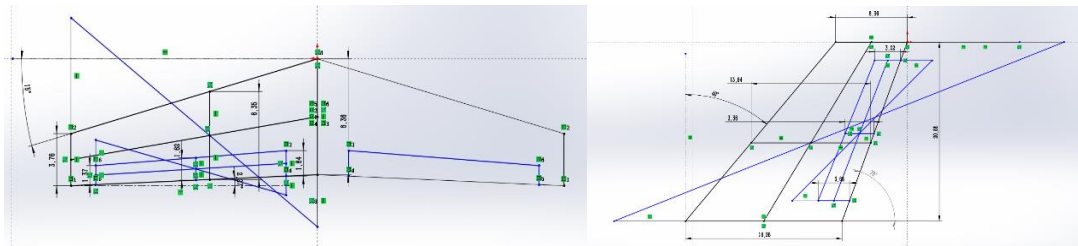
Vertical tail: 77.836kg

Also connected to the fuselage, the quality is 87.5% of the original mass, is 68.107kg.

4.5.4 Rudders and Elevators

The aircraft is a small general aviation aircraft. Therefore, it is designed to have a rudder area of 0.705 m² and a relative vertical area of 26.01%.

The elevator area is 0.876m². The relative flat area is 35.84%.



p. 4.5.1 tail plan view size

The average aerodynamic chord length of the elevator is 0.162m, relative chord length = 25.51%

The rudder average aerodynamic chord length 0.336m, relative chord length = 24.10%

4.5.5 Airfoil

As far as possible to reduce the increase in the area of the flat tail, using a large aspect ratio, a higher ratio of the heel to the tail, the critical tail M is greater than the wing, increase the dihedral dihedral, symmetrical airfoil, flat tail and vertical tail thickness

position before and after Staggered layout. Horizontal tail: NACA0009



The vertical tail requires large rigidity and heavy weight. The combination of the average relative thickness and the sweeping angle of the vertical tail is the same as that of the flat tail, which satisfies the occurrence of the shock wave and the wing on the

vertical tail surface. In addition to having higher resistance to diverge M number and aerodynamic efficiency, it has greater stall side slip angle and good stall characteristics, and makes the rudder surface have a higher rudder efficiency and a small hinge moment.



Vertical tail NACA0010

4.5.6 CATIA

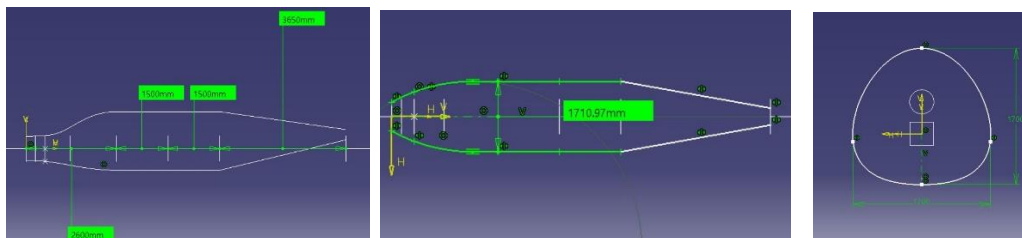


p. 4.5.2 tail space model

4.6 Fuselage

After fully investigating the existing four to six aircraft fuselage parameters of the existing general aircraft, by adding and averaging the average length of the four and six seats, the difference between the length of the four and the six seats is 1.5m, considering the design requirements of the 75% common weight between the four and six seats. Finally, the length of the four aircraft was 7.75m, and the length of the six aircraft was 9.25m.

Considering that the aircraft is single engine layout and motor should be placed in the head, so the longitudinal and transverse sections of the fuselage are determined, as shown in P.3.6.1 and Figure 3.6.2.



p. 3.6.1 fuselage three-view drawing

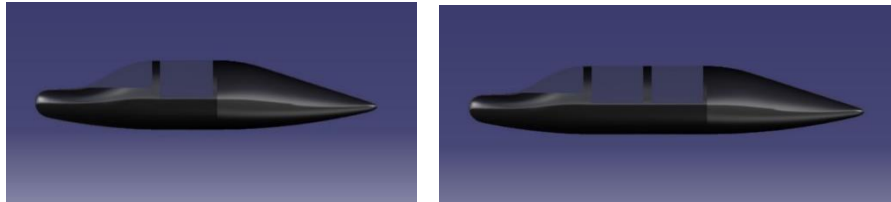
According to the draft of CATIA, the maximum section area, as shown in Figure 1.3, is 2.286 m² by CATIA.

According to formula $d_F = \sqrt{\frac{4A_F}{\pi}}$, we can get $d_F = 1.706$. Then, according to the slenderness ratio formula $\lambda_F = l_F / d_F$, the

fuselage slenderness ratio of the four aircraft can be obtained $\lambda_F = 4.54$, and the slenderness ratio of the six aircraft fuselage is

$\lambda_F = 5.4$.

The final airframe is shown in figures 1.4 and 1.5.



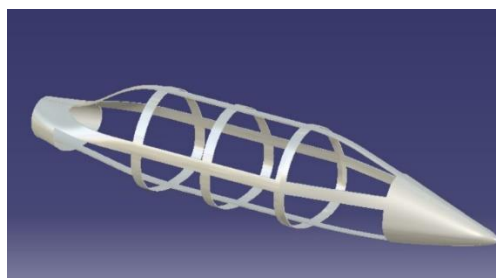
P. 3. 6. 4 Four-seats and six-seats fuselage

Material selection and weight estimation for each part of the fuselage

Body skin thickness	2.5mm	Fuselage skin material	carbon fiber
Six-seat skin volume	0.055m ³	Fuselage skin weight	71.5kg
four-seat skin volume	0.046m ³	Fuselage skin weight	59.8kg
Panoramic skylight thickness	0.046m ³	equivalent density	1*10 ³ kg/m ³
Six-seat glass volume	0.048 m ³	Glass weight	48kg
Six-seat glass volume	0.031m ³	Glass weight	31kg
fuselage structure material	10%aluminium alloy 2024, 10%aluminum lithium alloy 8090、80%carbon fiber	equivalent density	1.98*10 ³ kg/m ³
Six-seat Fuselage volume	0.102m ³	Six-seat Fuselage weight	201.8kg
four-seat Fuselage volume	0.085m ³	four-seat Fuselage weight	168.3kg
Total weight of six-seat fuselage	321.3kg	Total weight of four-seat fuselage	259.1kg

4.6.1 The fuselage structure layout design

Considering that the front fuselage and the middle fuselage need to be arranged the panoramic skylight, which is equivalent to the upper open mouth of the fuselage, the front fuselage and the middle machine should adopt truss beam structure. The structure is characterized by a strong longitudinal truss. The truss girder has a large interface, but the truss is very weak. Even the stringer can be discontinuous and the skin is thinner. After considering the three aspects of the best bending moment, the strengthening of the large opening structure and the transfer of the concentrated load, four longitudinal beams are arranged at the bottom, the upper part, and both sides of the panoramic skylight. In this way, the axial force caused by bending is mainly supported by truss girder, and the skin and long truss only bear a small part of axial force. At the same time, the position of the panoramic skylight is arranged between the two truss beams, which will not significantly reduce the bending strength and stiffness of the aircraft, and the mass increase caused by the opening reinforcement is less. Fig. 1.6 is the effect diagram of the main load-bearing structure of the six aircraft fuselage.



p. 3. 6. 6 The main bearing structure



p. 3. 6. 7 panoramic skylight opening status

Among them, the panoramic sunroof of a plane is divided into two halves, which rotates around the longitudinal girder at the top of the fuselage to play the role of the hatch door. The opening window of the panoramic skylight is shown in Figure 1.7.

At the same time, in order to meet the 75% generality of the 46 aircraft, the middle machine is designed to be a replacement part, and the structure of the front and rear fuselage of the 46 fuselage is the same, only the middle fuselage changes. In this way, it can not only meet the 75% General requirements, but also because the wing is arranged in the middle fuselage, changing the location of the wing of the four/six-seat aircraft can ensure that the same wing can be used for both four and six seats aircraft, further guaranteeing the requirements of generality.

Statistics of the common and non-shared parts of the aircraft can be used to estimate the generality.

	Propulsion System	Airframe
General part	whole (Motor, engine, and other) weight: 175.4kg	The front section of the fuselage, the tail section of the fuselage, the wing Flat tail, tail end, landing gear weight: 505.3kg
None general part	none	Middle fuselage Four-seat: 70.3kg six-seat: 132.5kg
System generality	100%	Four-seat: 87.8% six-seat: 79.2%
Total generality	Four-seat plane: 90.6%	six-seat plane: 83.7%

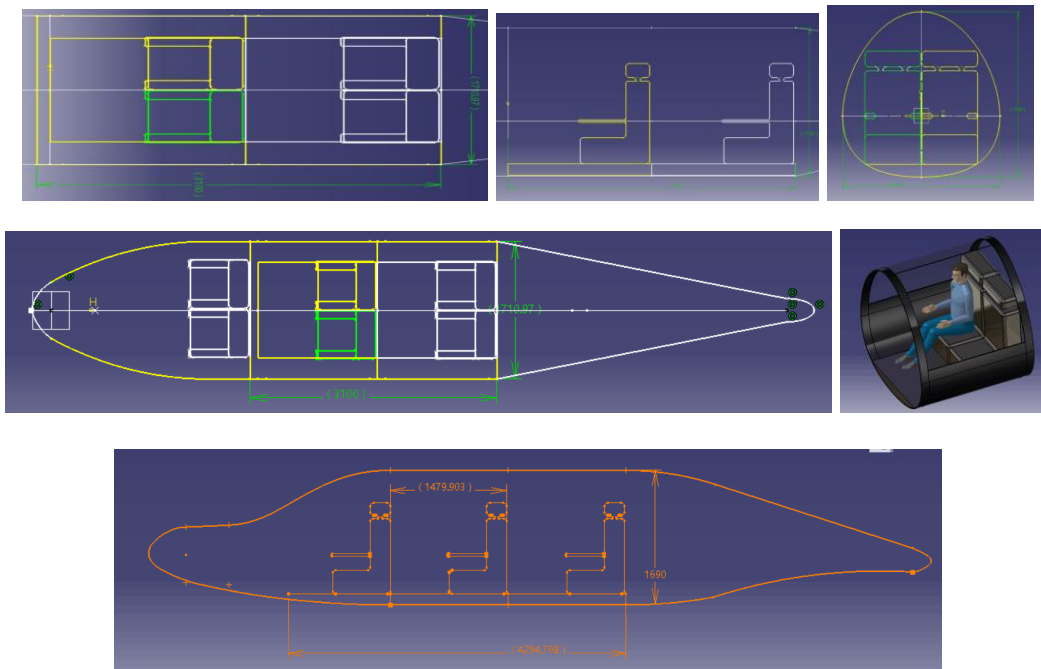
Through calculation, the generality of the four seats airplane is 87.8%, and the generality of the six seats airplane is 79.2%,

which satisfies the generality requirements of 75%.

4.7 Landing Gear

4 seats	Model	Level	Tire Type	Tire Diameter/mm	Section width/mm	Weight/kg
Main landing gear	20.5*6.75-10	12	TT	51.979	17.408	38.474
Front landing gear	6.00-6	4	TT	41.584	13.927	6.805
Weight/kg	45.279					
6 seats	Model	Level	Tire Type	Tire Diameter/mm	Section width/mm	Weight/kg
Main landing gear	21*7.25-10	8	TT	54.066	18.008	4.804
Front landing gear	6.00-6	6	TT	43.253	14.407	7.570
Weight /kg	50.374					

4.8 Main cabin



p. 4. 8. 1 cabin plan view size

4.9 Power System Design

4.9.1 Selection of engine and electric motor

The choice of engine and motor is based on our aircraft's power. The calculation of power depends on the important process in designing the mission profile. Now we rely mainly on the cruising process and take-off climb.

	Oil output/Max output	Elec.output/Max Output	Four seats time(min)	Six seats time(min)
Take-off	1	1	0.5	0.5
Climb	1	1	4	4.5
Await	0.2	1	12	12
Climb	1	1	4.5	5
Cruise	0.6	1	45	30
Decline	0	1	12	14.5
Sightseeing	0.3	1	170	100
Climb	1	1	8.5	9.5
Cruise	0.6	1	45	30
Decline	0	1	12	14.5
Await	0.2	1	15	15
Decline	0	1	5	5.5
Landing	0	1	0.5	0.5

The figure above is based on our preliminary fuel consumption and power consumption characteristics. From the figure we can see that in order to improve economy and reduce the noise of power system, we try to maximize the electronic power output value, which is also in line with the principle of economic and environmental protection.

According to the estimation method of fuel consumption for flight in the literature, we calculate the resistance, speed change and the power according to conservation of energy.

Take-off: take-off distance = 420m, airport altitude = 100m, runway friction coefficient = 0.05

Climb: initial height \approx 100m, stop height = 2000m, initial speed = 0.15Ma, stop speed = 0.25Ma

Cruise: Cruise Height = 4900m, Cruise Speed = 0.32Ma, Cruise Distance = 300km

Below we will analyze the power consumption of important processes step by step:

1. Take-off climb

At this stage, the energy of the aircraft mainly has such a few flows: incremental kinetic energy, incremental gravity potential

energy, and aerodynamic drag dissipation. $P_1 = W_0 v_y + \frac{W_0}{K} v_d + \frac{\Delta E_k}{Time}$ Calculate according to the design requirements of six seats, the take-off weight is $W=1847.03\text{kg}$. During the take-off process, we choose the aircraft's lift-drag ratio to be 10 (cruise lift-drag ratio is 12). This is on the lift characteristic curve of the selected airfoil, which is obtained and estimated by aerodynamic method. Because the final climb height is 4900m, the length of time in this phase is $Time = \frac{h}{v_y} = \frac{4900m}{6.604m/s} = 741s$. After leaving the ground, the aircraft speed is 31m/s, and sub-cruise speed (0.24Ma). The power calculated is 255.17kW.

Taking the loss of machinery and the efficiency of the conversion of the propeller into account, we also need to consider that the density in the air becomes smaller, the change in the speed of sound caused by the sound speed, and the aerodynamic drag power in the flight process increases with the speed. To sum up the factors above, we now make conservative estimates with an efficiency of 0.85 and find that we use the power system 300kW as the basis for calculation. Because of the full load work of oily and electric

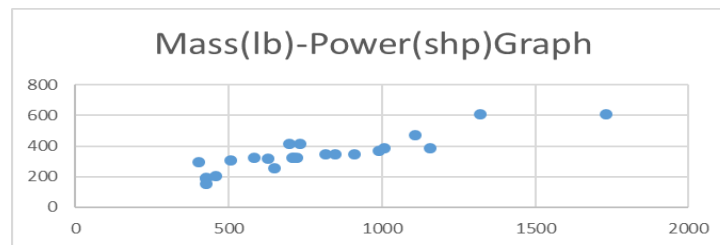
engine during take-off process, here is output power: $P_{oil} + P_{electric} = 300kW$

2. cruise phase

The cruise phase only involves overcoming air resistance. We will calculate the air resistance power when cruising:

$P=151.083\text{kW}$. Here we choose the maximum lift-to-drag ratio to reduce fuel consumption. Similarly, according to the design requirements of the four seats, we calculated that the four-seat aircraft had a take-off power requirement of 175.946 kW (206.995 kW), and the four-seat aircraft had a cruise power requirement of approximately 126.5135 kW (148 kW), which was lower than the six-seat aircraft requirement. To ensure the universality of the 7-seat plane and the 6-seat plane is 75%, we will use the 6-seat plane as a reference for future calculations.

We query the data and draw the scatter plots of the engine's power and quality as follows:



After the linear regression, we obtained a growth ratio of $0.396233\text{ lb/shp}=0.244528268\text{ kg/kW}$, estimated according to a motor output of 50 kg and 260 kW , the power of the oil generator is x , and the power of the motor is y . The total mass control equation is $z = z_0 + 0.244528x + 0.1923y$.

So we calculated the mass fluctuation range of $57.69\text{-}73.3584\text{kg}$, then add the intercept of the mass power scatter plot $z_0=113\text{lb}=51.14\text{kg}$, we can get our power system quality at $108.83\text{-}124.4984\text{kg}$, here we choose The motor is calculated according to the most advanced Siemens motor, so we need to multiply a certain correction factor, after our attempt to multiply by 1.3 (the actual process through the statistics of the motor's ratio to get the expression of the control equation), so we are The power system is selected within the range of $141.479\text{-}161.84792\text{ kg}$.

In this case, we consider the power consumption of the cruise phase. After several attempts, we modify the original ratio. The ratio of oil and electricity for cruising is $0.6:0.52$ (the ratio here refers to the oil output of the oil. The maximum power of the motivation is 0.6, and the electric power accounts for 0.52 of the maximum power. The purpose of this selection is to adjust the

ratio of oil and electricity so that the overall efficiency is optimal and the quality is as small as possible.

So we list the equation

$$\begin{cases} x + y = 270kW \\ 0.6x + 0.52y = 151.083kW \end{cases}$$

The motor power is 136.4625kW, divided by the conversion efficiency of 0.9, and for the engines available on the market,

we finally get the required engine power of 150kW and the motor power of 150kW.

MODEL	COMPRESSION RATIO	HP	RPM	TBO	HEIGHT (IN)	WIDTH (IN)	LENGTH (IN)	DRY WT	REMARKS
IO-360-B	8.70:1	200	2,700	2000	19.35	34.85	29.81-31.33	324-335	Dynafoal Mounts
AEIO-360-A	8.70:1	200	2,700		19.35	34.25	29.81	299	
AEIO-360-B	8.70:1	180	2,700		24.84	33.37	29.81	275	
L/IO-360-C	8.50:1	180	2,700	*	20.70-24.84	33.37	29.81-32.81	290-308	Dynafoal Mounts
IO-360-F	8.70:1	200	2,700	2000	19.48	34.25	29.81-33.65	319-329	Dynafoal Mounts
IO-360-J	8.50:1	180	2,700	2000	20.70	33.37	32.09	303	Dynafoal Mounts
IO-360-L	8.70:1	200	2,700	2000	19.35	34.25	31.33	323-330	Dynafoal Mounts
IO-360-M	8.50:1	160	2,400	2000	24.84	33.37	29.81	278	Dynafoal Mounts
TIO-360-A	8.50:1	180	2,700	2000	20.26	33.38	32.75	300	Dynafoal Mounts
TIO-360-C	7.30:1	200	2,575	1200	19.92-21.34	34.25	34.25	389-407	Dynafoal Mounts
	7.30:1	210	2,575	*	21.65	19.09	35.82	379	Dynafoal Mounts
IO-390-X									
	8.70:1	210	2,700	2000	19.35	34.25	30.70	308	Dynafoal Mounts
IO-580-B									
	8.90:1	315	2,700		21.04	34.25	39.34	444	
IO-720-A									
IO-720-B	8.70:1	400	2,650		22.53	34.25	46.06-46.41	597-601	
IO-720-D	8.70:1	400	2,650		20.63-20.88	34.25	46.08-47.97	593	
* Depends on configuration	8.70:1	400	2,650		22.06-22.11	34.25	46.41-46.80	593-607	

Contrast performance we chose the higher performance Lycoming AEIO-360-A four-cylinder piston engine. The

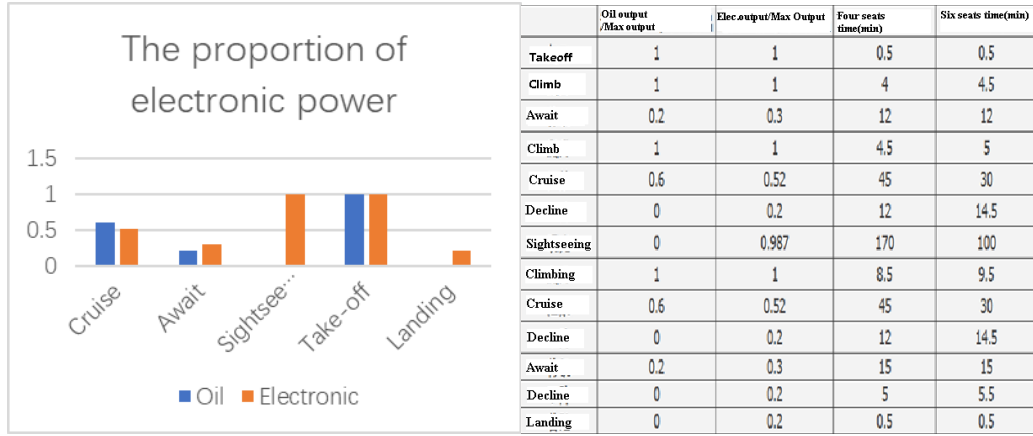
important parameters are as follows: Power 200HP Speed 2700r/min Height 19.35inch Width 34.25 inch Length 29.81 inch Dry weight 299LBS (135.62341kg).

For the electric motor, we have inquired that Siemens has a motor with a mass of 50kg and a power of 260kW. Therefore, we can find that the mass of the engine of 150kW is about 28.846kg, and the efficiency of the motor is 95%.

Sightseeing can use electricity completely for the sake of play. At the lowest cruising speed, we use electric energy supply, so

we get: The electric power accounts for the maximum 0.987. The other same way can be calculated:

Item	Oil proportion	Electronic proportion
Cruise	0.6	0.52
Await	0.2	0.3
Sightseeing	0	0.987
Take-off	1	1
Landing	0	0.2



Here, we give the efficiency of the electric system: the components of the electric system are divided into electric motors

95% (provided by Siemens), the current efficiency of the fuel cell is 0.7, so the total efficiency of the electric system is 0.665.

4.9.2 Calculation of fuel consumption

First, it is estimated according to the energy: the fuel density of the Lycoming engine is 0.7214g/cm^3 , and the thermal value of the gasoline is $4.3 \times 10^7 \text{ J / kg}$. We consider the impact of heat engine and mechanical efficiency, we choose

35% efficiency, according to the power of the engine is 150kW we list the formula:

$$sfc = \frac{Pt}{Q\rho\eta} = \frac{150 \times 3.6 \times 10^6}{4.3 \times 10^7 \times 35\%} = 35.88 \text{ kg / h}$$

The total fuel volume can be programmed to calculate the sum of power and time at each stage, With the weight of 0.06 dead oil, six seat 37.657kg and four 47.54948kg.

4.9.3 Hydrogen mass estimation

According to the conservation of energy, almost all of our aircraft's flight profile is put into use. Therefore, the hydrogen quality estimate is relatively simple. We assume that the entire journey is calculated according to the power of sightseeing, that is, 100kW, and then we multiply the time. Here we use the maximum flight time. 6h (1800km flight distance except cruising speed) according to caloric value of hydrogen: $4.7 \times 10^8 \text{ J / kg}$. We can calculate that the hydrogen quality is 4.5957kg in order to leave a certain margin, and consider the corresponding loss, we get 5kg of hydrogen storage. However, we chose an electric system with an efficiency of 0.65 so we need a quantity of 7.692 kg of hydrogen.

According to the density of liquid hydrogen 0.07g/cm^3 , we calculated that we need a hydrogen tank of 109.89L , which is about 130L . According to the data we inquired, the hydrogen tank of “hydrogen 1” of the existing GM company can be Stores 5 kg (75 L) of liquid hydrogen, including a total of 95kg of heat management system Liang Yi, Wang Wei, Guo Youyi, et al. Development status and prospects of liquid hydrogen storage tanks for hydrogen vehicles[J]. Cryogenics, 2001(5)): 31-36. Referring to the above table, we can estimate that the inner diameter of the required 130L hydrogen storage tank can be taken as 0.4m , the height is 0.211m , the total weight plus liquid hydrogen is 40kg (liquid hydrogen density is 0.07g/cm^3 , Weight 9.1kg) This size will have a big impact on the overall layout.

4.9.4 Final choice of fuel cell

Considering the requirements of aircraft quality, we cannot carry pure oxygen, so it is best to use the introduced air as an oxidant. In order to reduce the energy consumption of the heat pipe management system, we chose a proton exchange membrane fuel cell to be able to operate at room temperature.

Referring to the battery usage of existing fuel cell vehicles, we can see that the highest power density is 3.1kW/L and 2.0kW/kg . Therefore, the fuel cell has a mass of 75kg and a volume of 45L because the fuel cell can be Multiple strings are connected in parallel, so the shapes can be more varied. The reference size is given here: $3*3*5\text{dm}$.

4.9.5 Reason and weight of lithium battery

We design the aircraft's power system energy source for fuel cells, while the fuel cell technology is relatively new, and the reliability is not high. The use of fuel cell power for avionics systems that are safe for aircraft flight does not guarantee its stability and safety. Therefore, we chose to use a mature lithium battery to power the aircraft avionics system.

We conducted reasonable planning and found that the higher the proportion of hydrogen, the lower the total mass, and because we need to use a lithium battery for avionics alone for safety and reliability reasons, we got my power scheme: the energy source of the power system is mainly Hydrogen fuel cells, and the avionics system is a lithium battery.

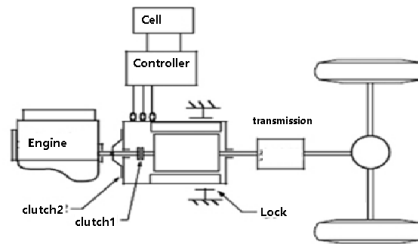
According to the lithium battery power density of 0.4kWh/kg, in accordance with the flight of 6 hours, arrange a certain margin, our avionics system working time is 8h, according to the power of 1kW, our lithium battery quality is 20kg.

4.9.6 Power Transmission System Design and Selection

The aircraft we chose is a single-engine hybrid aircraft. Here we place power systems such as the engine and the electric motor on the head of the aircraft. This leads to issues related to the power transmission and the size and center of gravity offset.

For this type of aircraft, it is important to consider selecting and designing a transmission suitable for this aircraft.

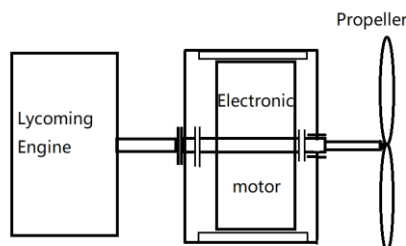
After reference, we learned that hybrid vehicles have torque-coupled power transmission systems, speed-coupled power transmission systems, and torque-coupled, speed-coupled hybrid power transmission systems:



p. 4.9.1 hybrid power transmission system

We will consider the size of the nose part of the space we will choose torque coupling and speed coupling hybrid power transmission system.

Explanation: We did not install a gear reducer for the propeller here, because according to the data we found, the existing Lycoming engine with appropriate power is about 2700 r/min. And when the mechanism is speed coupled, the rotation speed of the two will increase the efficiency of the propeller according to a certain proportion (Propeller efficiency calculation program analysis);



p. 4.9.2 propeller and engine system

The speed of the motor and the speed of the engine do not match, so we use this structure that can switch coupling. Among them, the engine speed is constant during normal operation, but the rotation speed of the motor is related to the input voltage. We installed the clutch on the torque-coupled coupler, using the clutch's damping action, and adjusting the input voltage at the same time, so that the rotation speed can be fully synchronized, which is similar to the car's engine and wheel drive. When coupled in accordance with the speed, the engine drives the permanent magnets to rotate, and the speed of the rotor relative to the permanent magnets is constant, so the output speed is a superposition of the two, which makes the output propeller can adjust the rotation speed to maximize the efficiency.

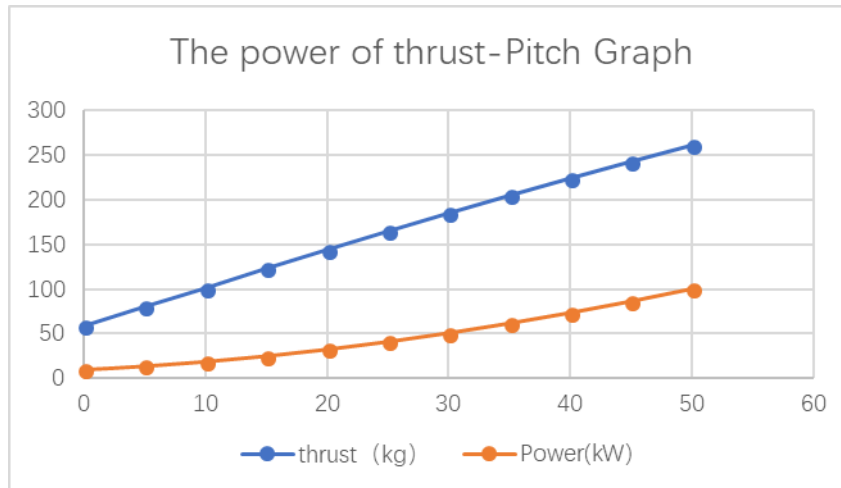
4.9.7 Propeller selection and parameter display

After inquiring to the data, we can find the existing propeller for power and speed:

	Maximum Power (HP)	Maximum Rotating Speed (r/min)	Diameter (mm)
2	80	2550	1620
3	100	2550	1660
4	80	2200	1730

We designed the aircraft to operate at the same time during the take-off process. During the cruising process, the motor was working (150 kW). Therefore, the speed range was approximately within the range of 2000-2700 r/min, and the power range was 100-200 kW because of the power. The bigger the diameter is, the bigger the diameter should be in order to increase the efficiency of the paddle. So we use this type of propeller to choose another company's propeller product; from these three sets of data we can find that the four-paddle aircraft is more suitable for our requirements. Select four-blade propellers in our designed aircraft

We have used our experience to choose a suitable propeller diameter of 78inch (approx. 100cm). In order to ensure that we can use the motor to drive the propeller, the output power is not more than 150kW, so we choose to use different speeds at different speeds. Pitch.



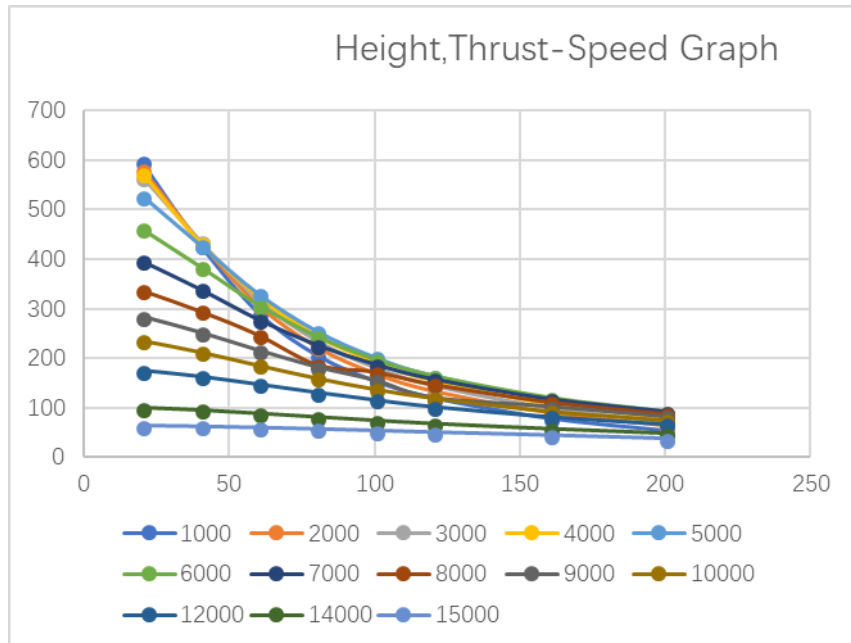
From the figure, it can be seen that with the increase of the pitch, the pulling force and the consumed power increase continuously. Therefore, in order to maintain the appropriate tension power, we must select the appropriate pitch. On the other hand, an increase in speed will affect the influence of the pitch on tension and power. The figure above shows the curve at speed standstill. At a cruising speed (approximately 100 m/s), the pitch will become very large.

In order to get the proper pitch, we use the parameter iterative method: through the professional propeller pull calculator, and through our constant changes to try the diameter and pitch, taking into account the tension, speed, efficiency and input and output power, select the following two Stage propeller parameters, as shown in the following table:

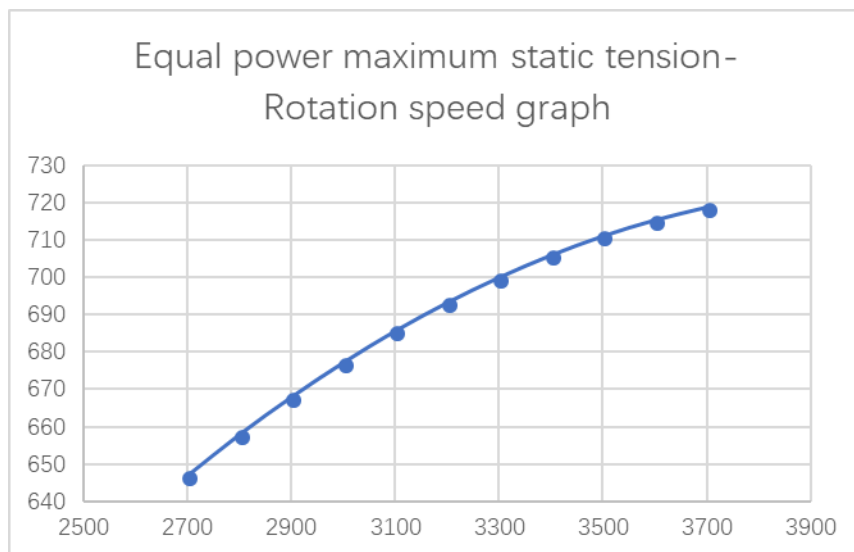
Variable pitch paddle parameter table

Item	airspeed km/h	Pitch Inch	Diameter Inch	Thrust Kg	Power kW	Efficient
Cruise	370.4	138	78	125.89	137.9	90.473
Take-off	0	6.41	78	440.07	135	0

Taking into account the changes in altitude and the pull-down forces at different speeds, the curves are as follows:



Note: Here we need to consider the effect of propeller rotation speed, which is generally expressed and related, according to the previously selected different coupling speed and torque coupling, because the power in order to meet take-off climb performance, so our engine power is larger, If you only use 2700rpm speed will not perform well: as shown below



Therefore, the above calculation needs to consider that the power speed changes according to the square root of the power

change, that is, here is an expression $\sqrt{\frac{P_1}{P_2}} = \frac{\omega_1}{\omega_2}$, When the speed is coupled, the maximum speed

is $2700 \times \sqrt{2} \approx 3800r / \text{min}$

4.9.8 Engine failure flight distance calculation

Engine failure, lift-to-drag ratio is calculated according to the cruising-drag ratio of about 12. Calculated according to four seats, the aircraft of 1550kg, the resistance is 129.16kg, (1265.8N) the energy of hydrogen is $2.35 \times 10^6 \text{kJ}$ and can maintain the flight of 1855.53km. Multiplied by the hydrogen energy conversion factor 0.450134 (the efficiency of the total energy flight distance and the actual flight distance), so the failure flight distance is 835.687km, where the distance is a conservative estimate, because the efficiency of the heat engine is much smaller than the fuel cell, so according to 0.450134 The efficiency is lower than the actual efficiency of the fuel cell. Therefore, the actual battery life is greater than 835km.

4.10 Advanced Technology

In order to enhance the highlights and competitiveness of our project, we decided to adopt a variety of new technologies on the aircraft. After discussion, we decided to apply the whole parachute, deicing system, and panoramic sunroof technology to our aircraft.

4.10.1 Whole Parachute

In order to optimize the safety performance of the aircraft and improve the survivability of the crew, we have installed a parachute of a small general-purpose aircraft on the aircraft. I have referred to many parachute systems that have already been put into use, and also to the aircraft on which this system is installed. After comparing, we finally found that the Cirrus company's extensive use of the parachute system in their aircraft is our ideal choice, and then we made relevant research to find out the detailed design of this system.

In order to improve the flight safety of small general-purpose aircraft, BRS Aviation designed a complete parachute system that has been installed on all Cessna 172, Cessna 182 and Cirrus aircraft. So far, APS has saved the lives of pilots and passengers in more than a hundred aerial special events, and its necessity and feasibility have been effectively verified. APS is our additional system, you can choose whether to install.



p. 4.10.1 different states of parachute

We need to determine the weight of the whole parachute system and other parameters to facilitate the overall design of the aircraft. According to the information obtained from the official website of BRS Aviation and Cirrus, we learned that the information on APS installed on Cessna 172 and Cessna 182 is as follows:

Aircraft Model	Maximum take-off weight	APS total weight	Parachute diameter and area	Parachute withstand overload	Parachute landing speed
Cessna172	1110kg	35.8kg	19.8m/223m ²	<4G	<8.4m/s
Cessna182	1406kg	38.6kg	19.8m/223m ²	<4G	<8.4m/s

From this we simply calculate the relevant parameters of our APS:

Aircraft Type	Maximum take-off weight	APS total weight	Parachute withstand overload	Parachute landing speed
Four seats	1517kg	(39.6±5) kg	<4G	<8.4m/s
Six seats	1780kg	(42.1±5) kg	<4G	<8.4m/s

Parachute related parameters:

Parachute diameter	Parachute area
19.8m	223m ²

4.10.2 anti-ice system

Our aircraft is a four-six-seat small general aviation aircraft. Considering the weight, working time and work energy consumption of de-icing devices, we have chosen the de-icing system to match our mission requirements. as follows:

Wing and tail: TKS anti-ice system

Propeller: Ice cast ring+ TKS anti-ice system
 Airspeed head: Electrothermal anti icing
 Front edge of engine inlet: Air heat anti icing

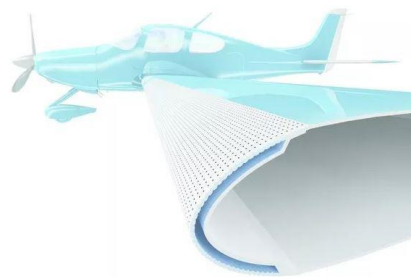
Our aircraft should not use high-power electric deicing equipment, so we need to use the TKS ice protection system in places where we need a large area of anti-icing, such as wings and empennage. In the narrow and complex structure of the pitot tube, taking into account its operating characteristics, we still use low-power electrothermal anti-icing. At the engine intake leading edge, in order to maximize efficiency, we decided to directly use gas-thermal anti-icing to recover waste heat.

Among them, the TKS ice protection system is a kind of deicing device widely used in small general aviation aircrafts. We have done relevant research and found a detailed design scheme for this system. The following is an overview and feasibility report we have concluded:

(1) TKS anti-ice protection system

The TKS anti-icing system is the preferred ice protection system (IPS) for most new general aviation and unmanned aircraft.

More than 6,000 aircraft are equipped with TKS.



Models	TKS Empty weight /kg	TKS Full weight (fluid-containing) /kg Storage	Storage Volume / L	Working Hours /h	Power
Cessna182	18.1	39	18.9	2	1.5 Amps @ 28 Volts during Normal Mode
Cessna 210	23.13	49.44	23.46	2.5	1.5 amps @ 28 volts during Normal Mode
Cirrus SR22 FIKI	27.21	60.78	30.3	2.5	3 Amps @ 28 volts during Normal Mode
Beechcraft	24.49	53.97	26.49	2.5	1.5 amps @ 28 volts

G36 FIKI					during Normal Mode
Skylark_4seats	23	50	24	2.5	1.5 amps @ 28 volts during Normal Mode
Skylark_6seats	25	55	27	2.5	1.5 amps @ 28 volts during Normal Mode

4.10.3 Panorama Skylight

The positioning of our aircraft is for sightseeing purpose. Therefore, in order to optimize the sightseeing effect and allow the crew to have the best viewing experience, we use the design of the panoramic sunroof. At the same time, this skylight is also the “door” of our aircraft. The skylight we eventually adopted The design is as follows:

(1) Stress layer

In order to ensure high breakage safety, multiple layers are selected for the force layer.

Considering that silicate glass is heat-resistant, resistant to media, and has a high surface hardness, it is suitable for use in areas with severe heating, abrasion resistance, and deicing requirements. However, the silicate glass reinforced by physical or chemical methods has a high compressive stress on its surface, which significantly increases the strength and thermal shock resistance of the material. Therefore, aerospace reinforced silicate glass (ordinary tempered glass) was selected as the stress layer.

(2) Protective layer

The protective layer is mainly used to withstand the impact of flying birds, to protect the safety of the use of electric heating layer, to ensure the safety of broken glass. Normal tempered glass has good thermal shock resistance, and the fragment is cubic particles when the tempered glass is destroyed, the higher the degree of tempering is, the smaller the particles are, and the visibility of the all-tempered glass is low, and the visibility of the semi-tempered glass is good. Therefore, semi-tempered glass was selected as the protective layer.

(3) Electric heating layer

At present, there are three types of electric heating layers. The tin oxide film has a firm film layer, the coating process is simple and mature, and the cost is low. There are many applications on airplanes at home and abroad. Therefore, the tin oxide film tends to be selected as the electric heating layer.

(4) Middle tier (glue layer)

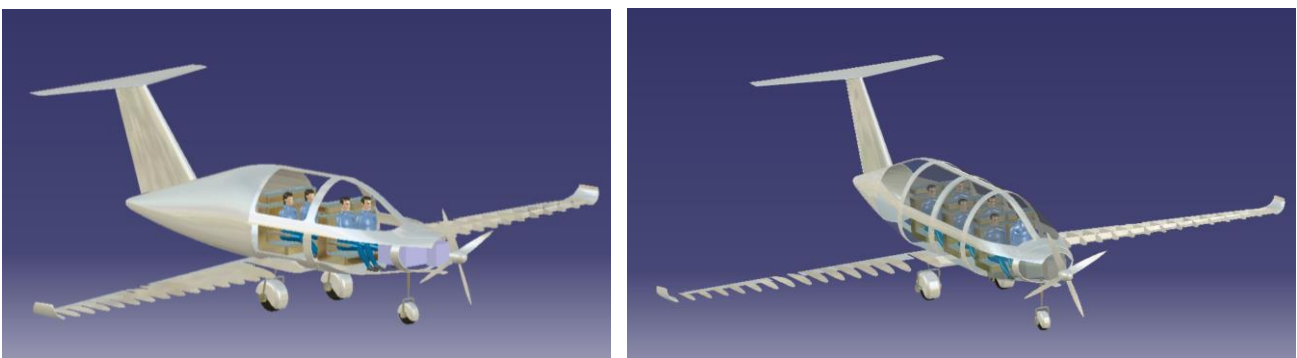
Considering the mutual compatibility, the conditions of use and the durability of the materials, the bonding layer selects the modified PVB interlayer (modified polyvinyl butyral interlayer), which has good adhesion and durability, and the operating temperature is -60o to 140o. Meet the standard "polyvinyl butyral (813) intermediate film" with a thickness of 2mm.

(5) Selection of wrapping material

Consider the use conditions and durability of the material, and use the degree of maturity to select the GS series wrapping material. The GS series wrapping material is a polyvinyl butyral resin and filler extruded by heating. It can be thermoformed and is suitable for the lamination of laminated glass made of polyvinyl butyral interlayer film. The process is slightly complicated. The use temperature is between -60o and 140o. The strength is higher than other wrapping materials, high durability, and good insulation.

Taking into account the high-altitude solar radiation, we are also preparing to install a one-way glass layer to reflect most of the solar radiation, giving the passengers the most comfortable ride experience. In addition, we also considered the color-changing glass used by the Boeing 787, but it was abandoned due to its complicated structure and high cost.

4.11 general arrangement



p. 4.11.1 four-seats six-seats aircraft inner structure

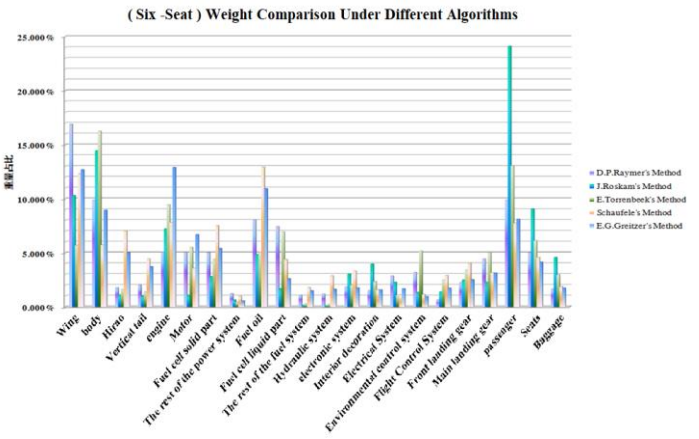
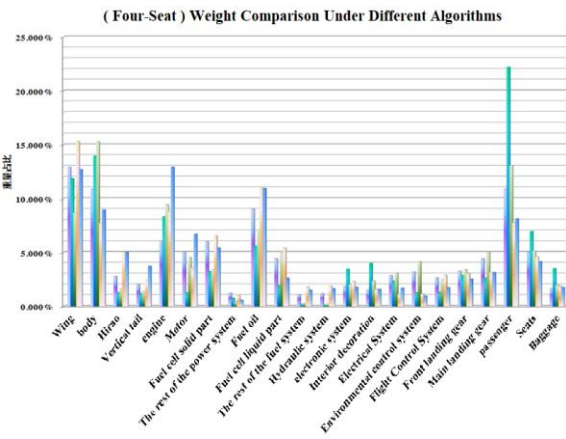
4.12 weight analysis

4.12.1 Approximate classification Gravimetric method

An approximate weight table of four or six seats can be obtained based on the Raymer estimate table: The external layout of the fuselage is involved in the gravimetric analysis process.

Four-Seat						Six-Seat					
	kg/m ²	Coefficient/m ² , kg	Center of Gravity/m	Coefficient	Result /kg		kg/m ²	Coefficient/m ² , kg	Center of Gravity/m	Coefficient	Result /kg
Wing	12	15.38	3.28	0.78	143.96	Wing	12	15.38	3.28	0.78	143.96
Horizon Tail	10	6.098	8.6	0.75	45.74	Horizon Tail	10	6.098	9.61	0.75	45.74
Vertical Tail	10	3.387	6.48	0.75	25.4	Vertical Tail	10	3.387	7.49	0.75	25.4
Body	7	31	3.56	0.85	184.45	Body	7	35.66	4	0.85	188.41
Landing Gear	0.057	前起: 1569.64*15% 主起: 1569.64*85%	1.6	0.88	11.41	Landing Gear	0.057	前起: 1847.03*15% 主起: 1847.03*85%	1.6	0.88	13.9
Engine	1.4	145	0.4	1	203	Engine	1.4	145	0.4	1	203
Other	1	351.06	3.56	1	351.06	Other	1	398.57	4	1	398.57
Motor	1	25	0.5	1	25	Motor	1	25	0.5	1	25
The Fuel Cell	1	49	0.7	1	49	The Fuel Cell	1	49	0.7	1	49
Weight /kg					1103.72	Weight /kg					1171.73
Center of gravity /m					3.536	Center of gravity /m					4.139

4.12.2 Statistical classification Gravimetric Method--comparison of four or six different algorithms



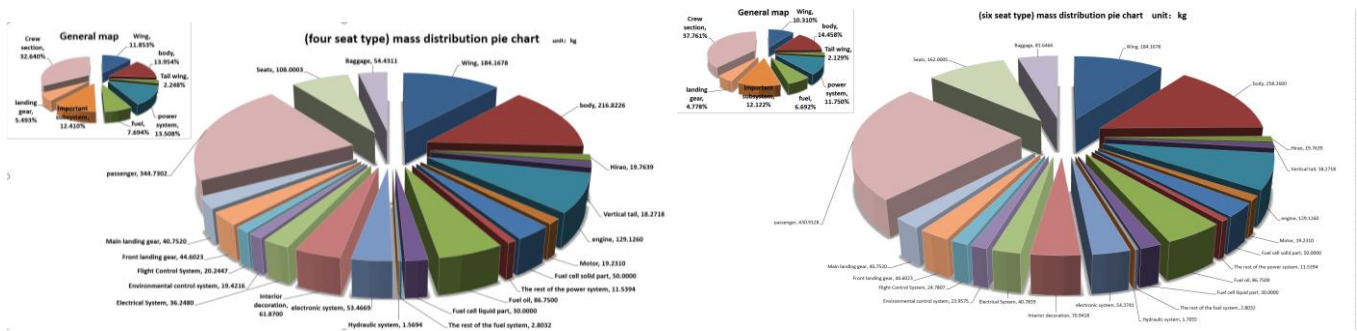
value as the 46-seat classification weight estimates, as shown in the following two figure:

Four seats										Six seats												
	Using composite materials			Center of gravity		product	Accounting					Using composite materials			Center of gravity		product	Accounting				
	Candy Coeff	Weight/lb	Weight/kg	From head/m	From Wing Long		From head/m	From Wing Long	From head/m			From Wing Long	Candy Coeff	Weight/lb	Weight/kg	From head/m		From Wing Long	From head/m	From Wing Long		
Wing	0.78	496.0200	184.2079	3.0314	0.8314	672.4700	11.8028	11.8028	center of grav	3.4676	Wing	0.78	496.0200	184.2079	3.0314	0.8314	746.1270	10.3109	10.3109	center of grav	3.9230	
body	0.85	678.9120	216.8228	3.7300	0.8600	820.2300	13.9548	13.9548			body	0.85	669.3700	238.2600	4.8530	1.2330	1157.0063	14.4585	14.4585			
Tail wing	0.73	43.3720	19.7639	8.6800	0.8000	171.4497	2.2488	1.1204			Tail wing	0.73	43.3720	19.7639	10.1950	6.9900	201.4932	2.1209	1.1006			
Vertical tail		40.2625	18.2718	7.1620	4.7625	138.1867	1.1106				Vertical tail		40.2625	18.2718	7.1620	4.3625	138.1867					
engine		284.6741	129.1200			159.7934	8.3100		Empty weight/kg	1437.0622	engine		284.6741	129.1200			159.7934			Empty weight/kg	1669.6267	
Motor		42.3971	19.2310			23.7984	1.2308				Motor		42.3971	19.2310			23.7984					
power system		110.2311	50.0000			41.9750	2.2108				power system		110.2311	50.0000			41.9750					
Fuel cell/wild part		25.4400	11.5394			11.5394	0.7474				Fuel cell/wild part		25.4400	11.5394			11.5394					
center of the power system		191.2310	86.7300			290.7340	5.5826		II load center	3.4089	center of the power system		191.2310	86.7300			290.7340			II load center	3.9212	
Fuel cell liquid part		66.1387	30.0000			100.5420	1.8018				Fuel cell liquid part		66.1387	30.0000			100.5420					
her rest of the fuel system		6.3800	2.8032			9.3946	0.4000				her rest of the fuel system		6.3800	2.8032			9.3946					
Hydraulic system		3.4600	1.5094			1.5450	0.1018		II load weight:	1833.8122	Hydraulic system		3.4600	1.5094			1.5450			II load weight:	1786.3769	
electronic system		117.8744	53.4660			0.7520	3.4818				electronic system		117.8744	53.4741			3.9550					
Interior decoration		136.4000	61.8700			245.9332	3.9828		12.1128		Interior decoration		136.4000	70.9418			4.3750			12.1128		
Electrical System		79.9132	36.2480			143.7234	2.2030				Electrical System		79.9132	36.2480			143.7234					
Environmental control system		42.8172	19.4218			27.0065	1.2206		Fly center of	3.4624	Environmental control system		42.8172	23.9575			4.3650			1.1650		
Flight Control System		44.8320	20.2447			80.2704	1.3030				Flight Control System		44.8320	24.7907			108.1676					
Front landing gear	0.88	98.3312	44.4923			1.2000	-1.4000		total fly weight	1507.1122	Front landing gear	0.88	98.3312	44.4923			1.2000			-2.0000		
Main landing gear		89.8427	40.7320			1.1650	2.6276				Main landing gear		89.8427	40.7320			3.9650			1.1650		
passenger		700.0000	344.7382			1227.2113	22.1800				passenger		800.0000	439.9128			4.3100					
Crew section		238.1000	108.0003			415.9013	6.9519				Crew section		257.1000	112.0003			1.1180					
Baggage		120.0000	54.4311			200.1592	3.5033		Automatic focus:	3.4812+0.341316	Baggage		180.0000	81.6466								
total		3425.5698	1553.8123			100.0000	100.0000				total		3938.2968	1786.3769			7004.4618			100.0000	100.0000	

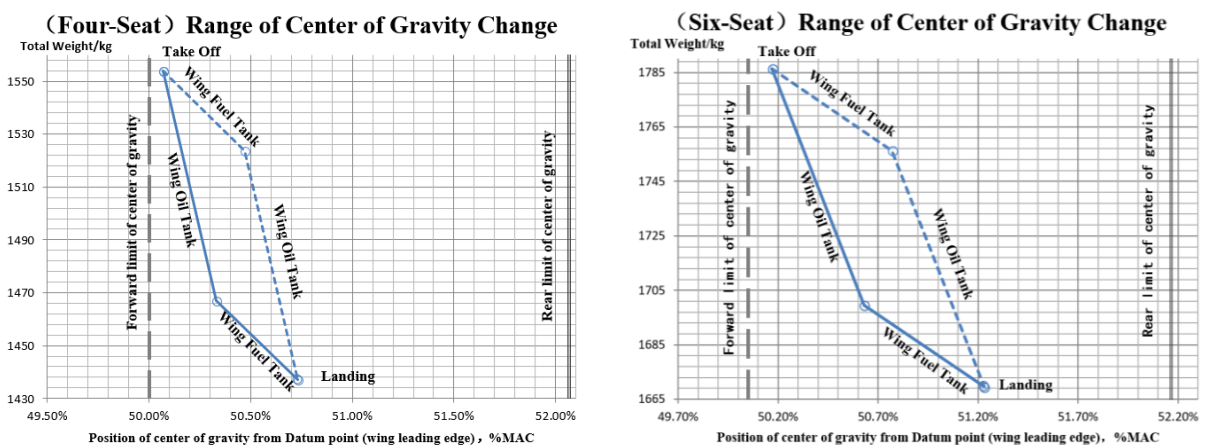
In the table, the specific weights of each major class and small class are given in detail. At the same time, it also gives the weight ratio of each large class and small group of components, it is convenient to build the concept of weight ratio and make the pie chart more convenient. The position of center of gravity of all kinds of components, including the position of the head and the position of the leading edge of the wing, The position of the distance nose is given to facilitate the calculation of the total center of gravity and the weight adjustment. The position of the leading edge of the airfoil is given to facilitate the calculation and

determination of the aerodynamic focus of the whole machine. In addition, the right side of the table also gives the empty machine weight, center of gravity, full load weight, center of gravity of the peaceful flying weight, center of gravity, which is given by the flying section.

At the same time, we can also give a 46-seat weight distribution of the pie chart, more convenient to see the weight of each component ratio:



After that, we can analyze the distribution of the length of each stage in the task profile and the analysis of maneuverability and stability to give the variation range of the center of gravity of the four and six blocks, the forward limit of center of gravity and the rear limit of center of gravity, as shown in Fig. Two, can be seen as follows: The change range of center of gravity is very small, meet the requirement of static stability margin, so meet flight requirement



5. Primary Performance analysis

5.1 Engineering estimates for aerodynamic characteristics

The data source for the calculation of lift characteristics is the design parameters and flight environment parameters of the aircraft. The calculation process refers to "Aircraft Design Manual Volume 6 - Aerodynamic Design". The lift characteristics are not changed for the wing and tailplane of the four or six seats. Basically the same, the following describes the engineering characteristics of lift characteristics:

5.1.1 Clean Configuration Lift characteristics

Flying Environment: $Ma=0.32$ $h=4900m$

(1) Wing lift characteristics (airfoil NACA2411)

$$\text{Related parameters: } \bar{x}_t = 29.5\% \quad \frac{t}{c} = 11\% \quad \tau = 20.4^\circ$$

1) Airfoil AoA of 0 lift

$$\alpha_0 = -2.5^\circ$$

2) Airfoil lift line slope

$$C_{l\alpha} = 6.28 + 4.7\left(\frac{t}{c}\right)(1 + 0.00375\tau) = 6.837 / rad$$

3) Airfoil maximum lift factor and corresponding angle of attack

$$C_{l_{\max}} = C_{l_{\max,ba}} + \Delta_1 C_{l_{\max}} + \Delta_2 C_{l_{\max}} + \Delta_3 C_{l_{\max}} + \Delta_4 C_{l_{\max}} + \Delta_5 C_{l_{\max}}$$

$$C_{l_{\max}} = 0.82 \quad \alpha_{C_{l_{\max}}} = 11.5^\circ$$

4) Wing AoA of 0 lift

$$\alpha_{0,w} = \left[\alpha_0 + \left(\frac{\Delta\alpha_0}{\tau_w} \right) \tau_w \right] \left(\frac{\alpha_{0,com}}{\alpha_{0,incom}} \right)$$

$$\alpha_{0,w} = -1.03^\circ$$

5) Wing lift line slope

$$C_{L\alpha,W} = \frac{2\pi A}{2 + \sqrt{\frac{A^2}{K^2}(\beta^2 + tg^2 \Lambda_{1/2})} + 4} = 5.570 / rad$$

6) Maximum lift coefficient of wing and corresponding angle of attack

$$\frac{4}{(C_l + 1) \cos \Lambda_{LE}} < A$$

So we use the following method to calculate:

$$C_{L_{max,W}} = \left(\frac{C_{L_{max}}}{C_{l_{max}}} \right) C_{l_{max}} + \Delta C_{L_{max}} \quad \alpha_{C_{L_{max,W}}} = \frac{C_{L_{max,W}}}{C_{L\alpha,W}} + \alpha_0 + \Delta \alpha_{C_{L_{max,W}}}$$

$$C_{L_{max,W}} = 1.503 \quad \alpha_{C_{L_{max,W}}} = 11^\circ$$

(2) Flat-tailed lift characteristics (airfoil NACA0009)

$$\text{Related parameters: } \bar{x}_t = 30\% \quad \frac{t}{c} = 9\% \quad \tau = 14.2^\circ$$

1) Airfoil AoA of 0 lift

$$\alpha_0 = 0^\circ$$

2) Airfoil lift line slope

$$C_{l\alpha} = 6.28 + 4.7 \left(\frac{t}{c} \right) (1 + 0.00375\tau) = 6.306 / rad$$

3) Airfoil maximum lift factor and corresponding angle of attack

$$C_{l_{max}} = C_{l_{max,ba}} + \Delta_1 C_{l_{max}} + \Delta_2 C_{l_{max}} + \Delta_3 C_{l_{max}} + \Delta_4 C_{l_{max}} + \Delta_5 C_{l_{max}}$$

$$C_{l_{max}} = 0.72 \quad \alpha_{C_{l_{max}}} = 12.5^\circ$$

4) Wing AoA of 0 lift

$$\alpha_{0,W} = 0^\circ$$

5) Wing lift line slope

$$C_{L\alpha,H} = \frac{2\pi A}{2 + \sqrt{\frac{A^2}{K^2}(\beta^2 + \operatorname{tg}^2 \Lambda_{1/2})} + 4} = 4.557 / \text{rad}$$

6) Maximum lift coefficient of wing and corresponding angle of attack

$$\frac{4}{(C_1 + 1) \cos \Lambda_{LE}} < A$$

$$C_{L_{\max,H}} = \left(\frac{C_{L_{\max}}}{C_{l_{\max}}} \right) C_{l_{\max}} + \Delta C_{L_{\max}} \quad \alpha_{C_{L_{\max,H}}} = \frac{C_{L_{\max,H}}}{C_{L\alpha,H}} + \alpha_0 + \Delta \alpha_{C_{L_{\max,H}}}$$

$$C_{L_{\max,H}} = 1.017 \quad \alpha_{C_{L_{\max,H}}} = 11.5^\circ$$

5.1.2 Full machine lift characteristics

(1) full machine lift line slope

$$C_{L\alpha} = C_{L\alpha,WF} + C_{L\alpha,H} \cdot k_q \left(\frac{S_H}{S} \right) \left(1 - \frac{d\varepsilon}{d\alpha} \right) = 5.570 / \text{rad}$$

(2) whole machine 0 L angle of attack

$$\alpha_{0,L} = (-C_{L0}) / C_{L\alpha} = -0.98$$

(3) full machine maximum lift factor and corresponding angle of attack

$$C_{L_{\max}} = C_{L_{\max,W}} - C_{L\alpha,WF} \cdot \Delta \alpha_{W/c} + C_{L\alpha,H} \left(\frac{S_H}{S} \right) \left[\alpha_{CL_{\max}} \left(1 - \frac{d\varepsilon}{d\alpha} \right) - \varepsilon_{0,H} + \psi_H \right] = 1.583$$

$$\alpha_{CL_{\max}} = \alpha_{CL_{\max,W}} - \psi_W = 11^\circ$$

5.1.3 Take-off and Landing configuration

(1) Take off ($\delta_f = 20^\circ$)

1. Increment of airfoil 0° angle-of-attack lift coefficient after flap deflection: $\Delta C_l = 1.066$
2. Slope of airfoil lift line after flap deflection: $C_{l,\delta}^\alpha = 7.681/\text{rad}$
3. airfoil maximum lift coefficient increment after deflection of flap: $\Delta C_{l_{\max}} = 0.730$
4. wing deflected by flaps 0° Angle of attack lift factor increment: $\Delta C_{LW} = 0.708$
5. the slope of the wing lift line after the flap deflection: $C_{LW,\delta}^\alpha = 6.12/\text{rad}$
6. Wing maximum lift coefficient increment after flap deflection: $\Delta C_{L_{\max,W}} = 0.336$
7. full machine after flap deflection 0° angle Lift factor increment: $\Delta C_L = 0.689$
8. the slope of the full lift line after the flap deflection: $C_{L,\delta}^\alpha = 7.623/\text{rad}$
9. maximum lift coefficient increment after flap deflection: $\Delta C_{L_{\max}} = 0.945$

Note: Take-off angle is set to Ten $^\circ$, at which point the lift factor is 1.834

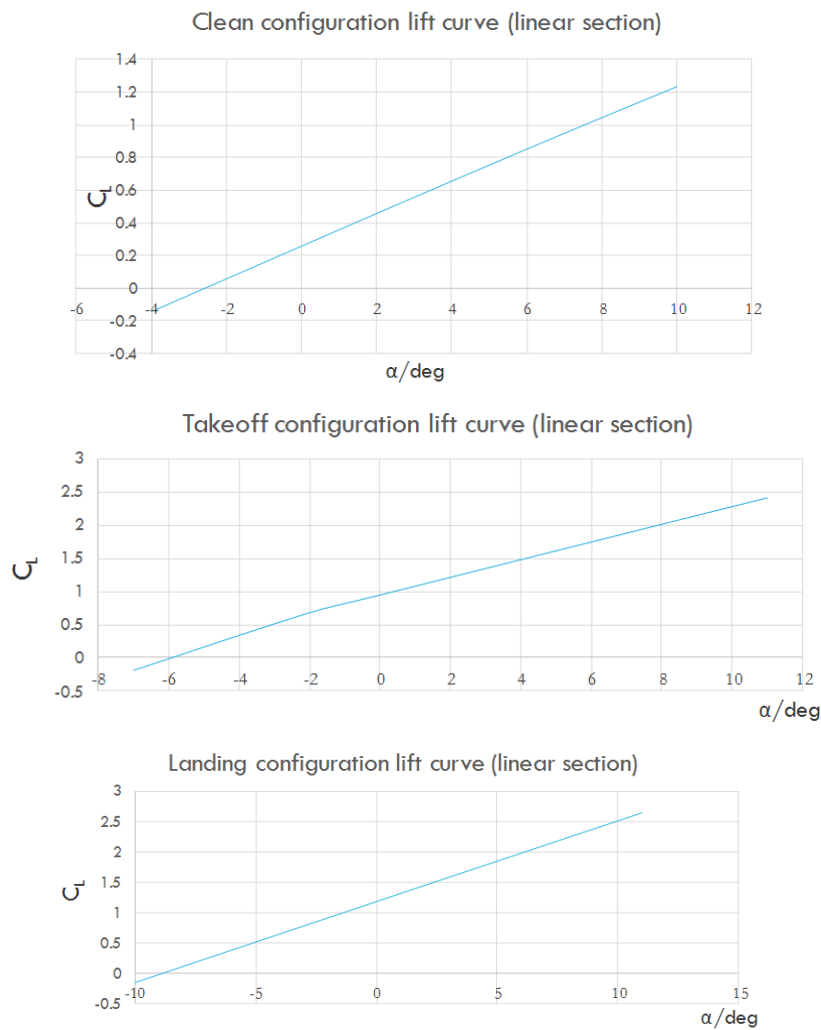
(2) Land ($\delta_f = 40^\circ$)

1. Increment of airfoil 0° angle-of-attack lift coefficient after flap deflection: $\Delta C_l = 1.492$
2. Slope of airfoil lift line after flap deflection: $C_{l,\delta}^\alpha = 7.681/\text{rad}$
3. airfoil maximum lift coefficient increment after deflection of flap: $\Delta C_{l_{\max}} = 1.102$
4. wing deflected by flaps 0° Angle of attack lift factor increment: $\Delta C_{LW} = 0.991$
5. the slope of the wing lift line after the flap deflection: $C_{LW,\delta}^\alpha = 6.12/\text{rad}$
6. Wing maximum lift coefficient increment after flap deflection: $\Delta C_{L_{\max,W}} = 0.507$
7. full machine after flap deflection 0° angle Lift factor increment: $\Delta C_L = 0.926$

8. the slope of the full lift line after the flap deflection: $C_{L,\delta}^\alpha = 7.623/\text{rad}$

9. maximum lift coefficient increment after flap deflection: $\Delta C_{L_{\max}} = 1.324$

Finally, we summarize the following table and draw the change curve of the whole machine lift coefficient with the angle of attack:



5.1.4 Resistance characteristics of clean configuration

In the process of calculating the resistance coefficient of the whole machine, we mainly calculate the formula and chart according to the teaching material, in addition, the relative formulae in the aircraft design manual are referenced in the calculation of the landing gear resistance performance.

Due to the flight performance of the flight envelope needs, we need to give different heights and different speed of the plane fly resistance coefficient, in order to find the required thrust. We selected 1000m to 12000m 10 Group elevation and 20m/s to 200m/s The eight group of speed calculations. The resistance coefficients of the take-off and landing configurations are calculated separately.

The first carries out calculations of the Reynolds number at different heights, velocities, and components. Then according to the various parts of different heights of different speeds of the Reynolds number in the textbook map 13.9 to get the friction coefficient of the flat plate C_F .

(1) Calculating the drag coefficient of the wing, flat tail and vertical tail

$$C_{D_{min,W}} = 2C_F \left[1 + 2\bar{t}_{av} + 100(\bar{t}_{av})^4 \right]$$

\bar{t}_{av} : Equivalent wing average thickness

C_F : Flat friction coefficient

Calculation results:

Wing minimum resistance coefficient								
	20	40	60	80	100	120	160	200
1000	0.010371	0.009013	0.008272	0.007902	0.007408	0.007284	0.0070374	0.006667
2000	0.010494	0.009136	0.008396	0.008025	0.007408	0.007408	0.0071609	0.006791
3000	0.010618	0.00926	0.008519	0.008149	0.007408	0.007531	0.0072844	0.006914
4000	0.010865	0.009383	0.008766	0.008272	0.007531	0.007655	0.0074078	0.007037
5000	0.011112	0.009507	0.008889	0.008272	0.007531	0.007778	0.0074078	0.007161
6000	0.014816	0.00963	0.009013	0.008396	0.007531	0.007902	0.0074078	0.007161
8000	0.014939	0.009754	0.009136	0.008766	0.008025	0.008149	0.0077782	0.007408
10000	0.015063	0.009877	0.009507	0.009136	0.008642	0.008396	0.0080252	0.007778
12000	0.158034	0.010865	0.010124	0.009507	0.00926	0.008889	0.0082721	0.008025

Flat tail minimum drag coefficient								
	20	40	60	80	100	120	160	200
1000	0.01452	0.00968	0.008954	0.00847	0.008228	0.007986	0.007381	0.007018
2000	0.014641	0.009801	0.009075	0.008591	0.008349	0.008107	0.007502	0.007139
3000	0.014762	0.009922	0.009196	0.008712	0.00847	0.008228	0.007623	0.00726
4000	0.014883	0.010164	0.009317	0.008954	0.008591	0.008349	0.007744	0.007381
5000	0.015004	0.010285	0.009438	0.009075	0.008712	0.00847	0.007865	0.007502
6000	0.015125	0.010406	0.00968	0.009196	0.008833	0.008591	0.008107	0.007744
8000	0.015125	0.010648	0.010043	0.009559	0.009075	0.008833	0.008349	0.007865
10000	0.015246	0.010769	0.010285	0.009922	0.009438	0.009075	0.008712	0.008107
12000	0.015609	0.015004	0.010769	0.010285	0.009559	0.009438	0.009075	0.008712

Minimum tail drag coefficient								
	20	40	60	80	100	120	160	200
1000	0.009255	0.008069	0.007713	0.007238	0.006882	0.006763	0.0065261	0.00617
2000	0.009492	0.008425	0.007831	0.007357	0.007001	0.006882	0.0066447	0.006289
3000	0.009611	0.008543	0.00795	0.007475	0.007119	0.007001	0.0066447	0.006407
4000	0.009967	0.008662	0.008069	0.007594	0.007238	0.007119	0.0067634	0.006526
5000	0.010086	0.008781	0.008187	0.007713	0.007357	0.007238	0.0067634	0.006645
6000	0.010204	0.008899	0.008306	0.007831	0.007594	0.007357	0.006882	0.006645
8000	0.010442	0.009137	0.008543	0.00795	0.007713	0.007594	0.006882	0.006645
10000	0.010679	0.009374	0.008781	0.008425	0.00795	0.007831	0.006882	0.006763
12000	0.014713	0.010086	0.009255	0.008899	0.008543	0.008306	0.0077126	0.007357

(2) airframe drag coefficient calculation

Equivalent diameter

$$d_F = \sqrt{\frac{4A_F}{\pi}}$$

Computer length ratio

$$\frac{l_F}{d_F}$$

airframe wetted area and maximum cross-sectional area ratio

$$\frac{S_{wet,F}}{A_F}$$

Calculation results

	Four seats	Six seats
airframe length, m	8.75	9.25
Maximum cross-sectional area, m ²	2.284338	2.284338
The maximum cross-sectional area of the fuselage, m	5.403	5.403

Equivalent diameter, m	1.705435	1.705435
airframe slenderness ratio	5.130655	5.423835
airframe wetted area and maximum cross-sectional area ratio	13.8609	17.2265

Calculate the zero-lift coefficient of the airframe

$$C_{d_{min,F}} = 1.02C_F \left[1 + \frac{1.5}{\left(\frac{l_F}{d_F}\right)^{3/2}} + \frac{7}{\left(\frac{l_F}{d_F}\right)^3} \right] \frac{S_{wet,F}}{A_F}$$

(3) Landing Gear Resistance Calculation

For a simple fixed landing gear, the landing gear we chose is a narrow pillar, unrectified landing gear, which is calculated with reference to the formula in the aircraft design manual. Resistance coefficient of main landing gear:

$$C_{D_{gear}} = C_{D_{\pi}} (W_t D_t / S)$$

Front landing gear drag coefficient:

$$C_{D_{gn}} = 0.5C_{D_{\pi}} (W_t D_t / S)$$

For narrow pillars without rectifying undercarriage, $C_{D_{\pi}}=0.52$, the width W_t , diameter D_t , referenced to the landing gear tire design table. The aircraft is a three-point landing gear layout consisting of two main landing gears and a nose landing gear.

Calculation results:

	Landing gear resistance coefficient
Four seats	0.0029
Six seats	0.0032

(4) Calculation of total drag coefficient

The drag coefficient of the whole machine is the sum of the drag coefficients of the components such as the wing, the tail, the tail, the fuselage, the landing gear, and so on. Considering that the reference area of each component is different, the overall drag coefficient is

$$C_{D_{min}} = C_{D_{min,W}} + C_{D_{min,H}} \frac{S_H}{S} + C_{D_{min,V}} \frac{S_V}{S} + C_{D_{min,F}} \frac{A_F}{S} + C_{D,t} \frac{S_t}{S}$$

$$C_D = C_{int} C_{Dmin} + k' C_L^2 + k'' (C_L - C_{L0})^2$$

There are two types of K's, formula and graph methods. Because the formula method is rough and does not take into account the influence of sharp cut ratios, the graphical method considers more comprehensive parameters. The specific parameters refer to the wing tail design. Refer to the chart method table on page 253 to obtain k'.

The coefficient of viscous flow induced resistance is used as the coefficient for k''. The viscosity-induced drag coefficient for both the wing and the tail can be taken as 0.01 when the initial estimate is made.

$$k' = (k')_W + (k')_H \frac{S_H}{S}$$

$$k'' = (k'')_W + (k'')_H \frac{S_H}{S}$$

Calculation results:

Full machine drag coefficient at different heights and speeds (four-seat type)								
Speed (m/s) \ Altitude (m)	20	40	60	80	100	120	160	200
0	0.5818	0.0509	0.0233	0.0187	0.0169	0.0163	0.0156	0.0148
1000	0.711	0.0589	0.025	0.0193	0.0173	0.0167	0.0159	0.0153
2000	0.8747	0.069	0.027	0.02	0.0176	0.0169	0.0162	0.0154
3000	0.9741	0.0752	0.0283	0.0205	0.0179	0.0172	0.0164	0.0156
4000	1.3509	0.0981	0.0329	0.022	0.0185	0.0176	0.0167	0.0159
5000	1.6931	0.1191	0.0371	0.0232	0.0191	0.018	0.0167	0.0161
6000	2.3217	0.1572	0.0446	0.0256	0.0199	0.0185	0.017	0.0162
8000	3.4799	0.2282	0.0583	0.0302	0.0222	0.0198	0.0177	0.0167
10000	5.6251	0.3601	0.0841	0.0386	0.0261	0.0216	0.0185	0.0175
12000	10.048	0.6254	0.136	0.0549	0.033	0.0253	0.0199	0.0183

Full machine drag coefficient at different heights and speeds (six-seat type)								
Speed (m/s) \ Altitude (m)	20	40	60	80	100	120	160	200
0	0.5834	0.0523	0.0246	0.02	0.0181	0.0175	0.0168	0.0159
1000	1.0047	0.0778	0.0295	0.0214	0.0189	0.0179	0.0171	0.0164
2000	1.2373	0.0921	0.0324	0.0223	0.0193	0.0183	0.0173	0.0166
3000	1.3783	0.1008	0.0342	0.023	0.0195	0.0185	0.0174	0.0168
4000	1.9133	0.1334	0.0407	0.0252	0.0205	0.0191	0.018	0.0171
5000	2.3991	0.1633	0.0464	0.0269	0.0213	0.0197	0.018	0.0173
6000	3.2897	0.2176	0.0571	0.0303	0.0225	0.0204	0.0184	0.0175
8000	4.9334	0.3185	0.0765	0.0364	0.0255	0.022	0.0192	0.018
10000	7.9772	0.5061	0.1132	0.0483	0.0309	0.0245	0.0202	0.0189
12000	14.185	0.8824	0.1868	0.0713	0.0401	0.0292	0.0218	0.0196

5.1.5 Landing configuration resistance characteristics

This process is mainly calculated with reference to the formula in the aircraft design manual. The resistance coefficient of the lifting device was mainly calculated, and the total resistance coefficient was added. The drag coefficient of the lifter consists of the following components:

$$C_{Dflap} = \Delta C_{Dprof} + \Delta C_{Di} + \Delta C_{Dint}$$

The first item is the increase in type of resistance of the booster device, the second item is the increase in lift resistance of the booster device, and the third item is the increase in the interference resistance of the booster device.

$$\Delta C_{Dprof} = (\Delta C_{dp, \Lambda_{1/4}=0}) \cos \Lambda_{1/4} S_{Wf} / S$$

$\Delta C_{dp, \Lambda_{1/4}=0}$: Two-dimensional increasing device type resistance increase;

$\Lambda_{1/4}$: Wing quarter chord swept angle;

S_{Wf} : The area of the wing belt lifting device part;

$$\Delta C_{Di} = K^2 (\Delta C_{Lflap})^2 \cos \Lambda_{1/4}$$

ΔC_{Lflap} : Increment of lift caused by booster;

$$\Delta C_{Dint} = K_{int} \Delta C_{Dprof}$$

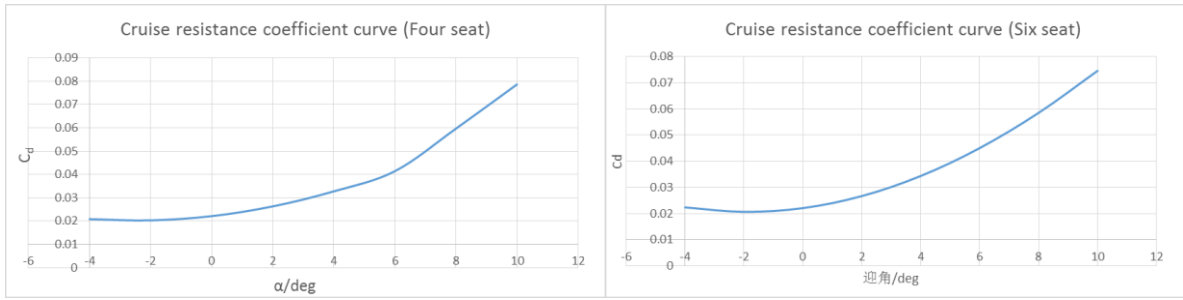
ΔC_{Dprof} : Increased type of resistance caused by a booster;

K_{int} : Increase the type factor of the device; (0 for simple flaps)

Calculation results:

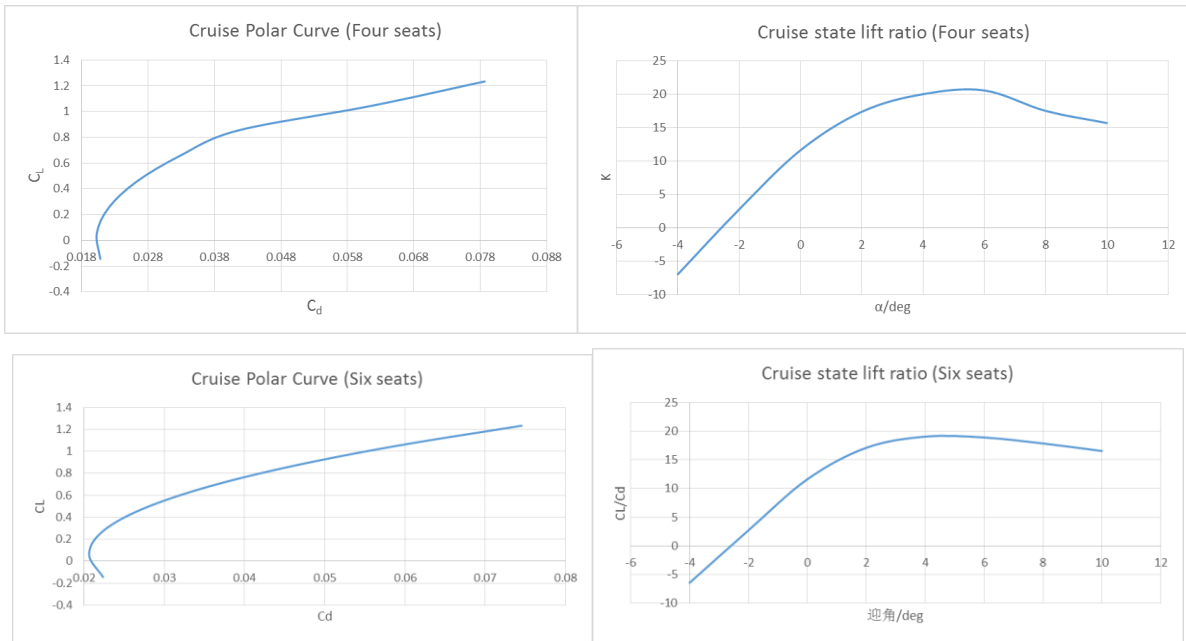
	Landing configuration drag coefficient (zero altitude)
Four seats	0.05093
Six seats	0.05234

Cruise resistance coefficient curve:

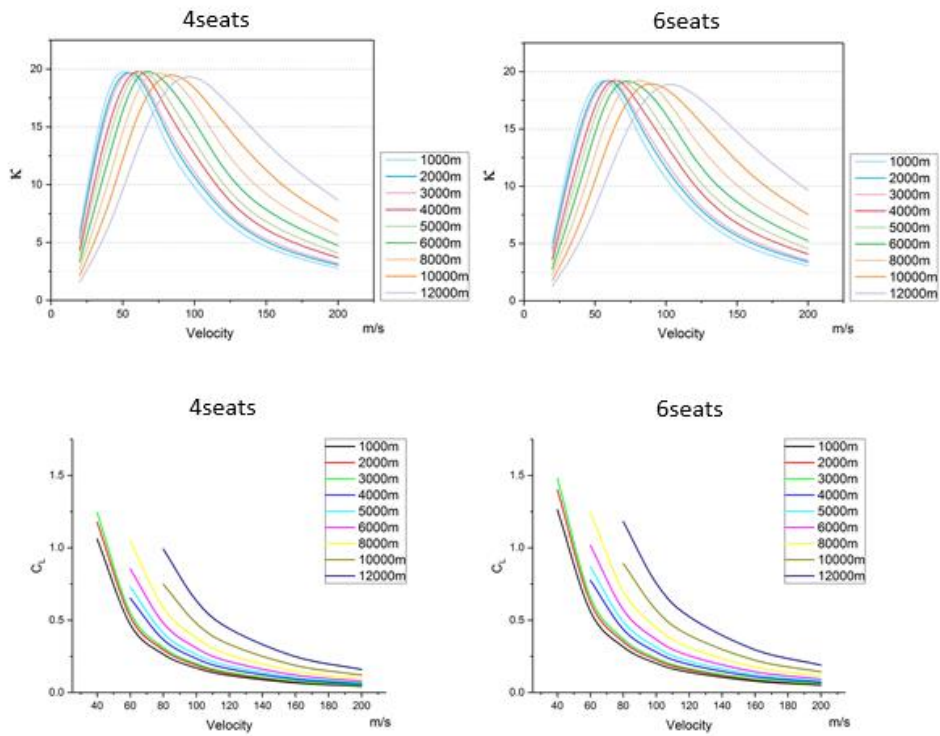


Cruising and lifting characteristics:

We got four or six cruising state polar curves and changes in lift-drag ratio with angle of attack:



The change of lift-drag ratio with speed and the change of lift coefficient with speed at different heights at different



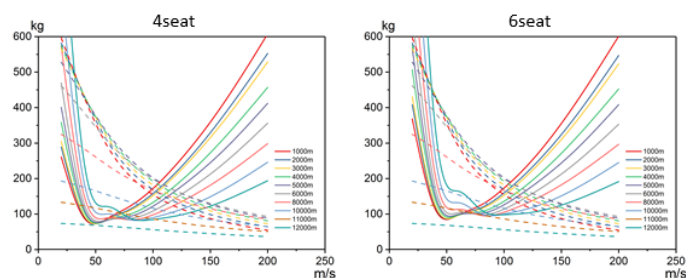
heights:

5.2 Flight Performance calculation

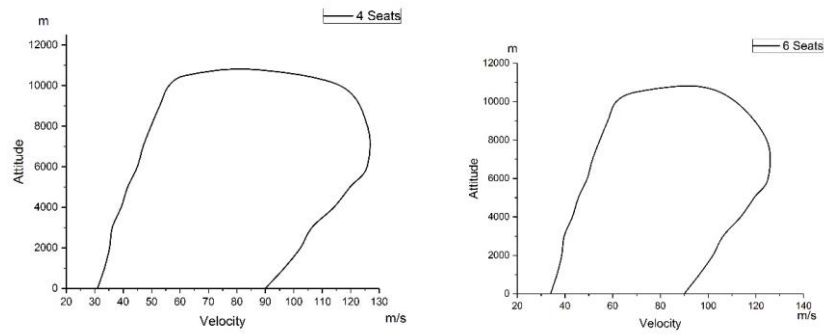
5.2.1 flight envelope and ceiling calculation

In this part, according to the calculation method given by textbook, the change curve of the available thrust with velocity and the change curve of thrust with velocity at different heights are obtained, the right intersection of the flight envelope at different heights is found, the left node does not exist or is much smaller than the stall velocity. So we use the stall velocity at different heights as the left edge of the flight envelope at different altitudes.

In order to calculate the theoretical ceiling of airplanes, we do not use the calculation methods listed in the textbook, but rather compare the left and right edges of the above, and when the two are equal, we think this is the theoretical ceiling of the aircraft. After constant attempts, we consider this height to be between the 10300~10500m, so that the flight envelope can be closed.



The above two figures are the use of aircraft at different heights with the thrust and available thrust with the speed of the change curve intersection, where the dotted line represents the available thrust, the solid line indicates the need for thrust, the same color to represent the same height. The final flight envelope is as follows:



5.2.2 Climb Performance

By Task cross section we know that throughout the flight we have a total of 3 a climbing segment in which the accelerated climb is taken after takeoff, and the two climbing segments are equal-speed climbs to the cruise altitude, so we calculate the following according to the textbook formula:

(1) Four -seats:

1. Accelerated Climb segment:

Starting altitude $\approx 100\text{m}$ Terminate Altitude $=2000\text{m}$

Start Speed $=0.09\text{ma}$ Stop Speed $=0.25\text{ma}$

Climb $V_{z,i} = 8.58\text{m/s}$

Climb Time $\Delta t_i = 3.69\text{min}$

Speed Change $\Delta V_i = 54.56\text{m/s}$

2. Start Altitude $=2000\text{m}$ Terminate Altitude $=4900\text{m}$

Speed $=0.25\text{ma}$

Climb $V_{z,i} = 5.83\text{m/s}$

Climb Time $\Delta t_i = 8.3\text{min}$

Climbing Angle $= 0.068\text{rad}$

Climb horizontal Distance $\Delta x_i = 705.11\text{m}$

3. equal-speed climbing segment two

Start Altitude $= 650\text{m}$ Terminate Altitude $= 4900\text{m}$

Speed $= 0.27\text{ma}$

Climb $V_{z,i} = 1.705\text{m/s}$

Climb Time $\Delta t_i = 28.3\text{min}$

Climbing Angle $\theta_i = 0.019\text{rad}$

Climb horizontal distance $\Delta x_i = 2609.55\text{m}$

(2) Six-seats:

1. accelerated Climb segment:

Starting altitude $\approx 100\text{m}$ Terminate Altitude $= 2000\text{m}$

Start Speed $= 0.1\text{ma}$ Stop Speed $= 0.25\text{ma}$

Climb $V_{z,i} = 7.97\text{m/s}$

Climb Time $\Delta t_i = 3.97\text{min}$

Speed Change $\Delta V_i = 51.15\text{m/s}$

2. equal-speed climb section one

Start Altitude $= 2000\text{m}$ Terminate Altitude $= 4800\text{m}$

Speed $= 0.25\text{ma}$

Climb $V_{z,i}=4.86\text{m/s}$

Climb Time $\Delta t_i=9.95\text{min}$

Climbing Angle $\theta_i=0.057\text{rad}$

Climb horizontal Distance $\Delta x_i=846.45\text{m}$

3. equal-speed climbing segment two

Start Altitude =650m Terminate Altitude =4800m

Speed =0.27Ma

Climb $V_{z,i}=1.42\text{m/s}$

Climb Time $\Delta t_i=34.04\text{min}$

Climbing Angle $\theta_i=0.015\text{rad}$

Climb horizontal distance $\Delta x_i=3133.47\text{m}$

5.2.3 Voyage and Airtime

According to the different stages of the task profile fuel consumption, hydrogen consumption rate we can calculate the weight change rate of the aircraft, and then according to the various stages of the planned flight time, based on the formula listed in the book to calculate the long voyage. At the same time, the maximum flight distance and the transition distance after the engine failure are calculated, and the standby voyage is also given.

	Four-seat airtime min	Six-seat airtime min	Four seats		Six seats		Four seat weight change rate (kg/h)	Four planned voyages (km)	Four seat weight change rate (kg/h)	Four planned voyages (km)
			Oil (kg)	Hydrogen (kg)	Oil (kg)	Hydrogen (kg)				
Take off	0.5	0.5	0.258333	0.006382979	0.258333	0.006382979	31.76595745	31.76595745	0.46035	0.5115
Climb	4	4.5	2.066667	0.05106383	2.325	0.057446809	31.76595745	31.76595745	7.3656	9.207
Standby	12	12	1.24	0.061276596	1.24	0.061276596	6.506382979	6.506382979	41.7384	42.966
Climb	8	10	4.133333	0.10212766	5.166667	0.127659574	31.76595745	31.76595745	46.6488	58.311
Cruise	45	30	13.95	0.292978723	9.3	0.195319149	18.9906383	18.9906383	294.84	196.56
Decline	12	14.5	0	0.030638298	0	0.037021277	0.153191489	0.153191489	72.4284	87.51765
Sightseeing	170	100	0	2.170212766	0	1.276595745	0.765957447	0.765957447	945.54	556.2
Climb	28	34	14.46667	0.357446809	17.56667	0.434042553	31.76595745	31.76595745	168.9996	205.2138
Cruise	45	30	13.95	0.292978723	9.3	0.195319149	18.9906383	18.9906383	294.84	196.56
Decline	12	14.5	0	0.030638298	0	0.037021277	0.153191489	0.153191489	69.9732	84.55095
Standby	15	15	1.55	0.076595745	1.55	0.076595745	6.506382979	6.506382979	52.173	53.7075
Decline	5	5.5	0	0.012765957	0	0.014042553	0.153191489	0.153191489	9.207	11.253
Landing	0.5	0.5	0	0.001276596	0	0.001276596	0.153191489	0.153191489	0.8334	0.9168
Total	357	271	51.615	3.48638298	46.707	2.52	90.75521902	106.8091513	2005.04775	1503.4752

Four seats type

Planned voyage: 2005.05km Total fuel consumption: 51.62kg
Total hydrogen consumption: 3.49kg

Planned flight time: 357min
Alternate range: 291.41km
Flight range: 2296.46km Total fuel consumption: 86.75kg
Total hydrogen consumption: 30kg

Engine failure flight distance: 960km

Six seats type

Planned voyage: 1503.48km Total fuel consumption: 46.707kg
Total hydrogen consumption: 2.52kg

Planned time: 271min
Alternate range: 399.96km
Flight range: 1903.44km Total fuel consumption: 86.75kg
Total hydrogen consumption: 30kg

Engine failure flight distance: 720km

5.2.4 Take-off and landing performance calculation

Take-off performance calculation reference to the textbook calculation method, different road conditions to take different friction coefficient, to get the Take-off performance under different ground condition, landing performance using the statistical method taught in the calculation.

at the same time, according to the course requirements of the elevation of zero and elevation as 5000ft the Take-off and landing performance of the.

Calculated results:

(1) Zero elevation

1. take-off speed calculation

Take-off angle of attack α : 10° Wiping corner: 15° CL, $\max=2.02$

		km/h	m/s
Four seats	V _r	115.457	32.07
Six seats		127.278	35.35

2. Take-off distance calculation

sea level				
Four seats		Regular runway (f=0.025)	Concrete ground (f=0.035)	Hard grass (f=0.085)
	L _{tot} /m	254.252	256.069	268.786
	L ₂ /m	57.499	57.499	57.499
	L ₃ /m	33.018	33.018	33.018

	L_{to}/m	344.768	346.586	359.302
Six seats		Regular runway ($f=0.025$)	Concrete ground ($f=0.035$)	Hard grass ($f=0.085$)
	L_{tor}/m	288.186	290.010	302.672
	L_2/m	57.499	57.499	57.499
	L_3/m	41.210	41.210	41.210
	L_{to}/m	386.895	388.719	401.382

3. Landing performance calculation

	V_A (m)	$L_L(m)$
Four seats	34.74	422.36
Six seats	38.30	513.27

(2) Altitude: 5000ft

1. Takeoff speed calculation

Take-off angle of attack α : 10° Wiping corner: 15° $CL_{max}=2.02$

		km/h	m/s
Four seats	V_r	127.636	35.454
Six seats		140.705	39.085

2. Take-off distance calculation

Altitude: 5000ft				
Four seats		Regular runway ($f=0.025$)	Concrete ground ($f=0.035$)	Hard grass ($f=0.085$)
	L_{tor}/m	254.181	257.519	278.027
	L_2/m	63.565	63.565	63.565
	L_3/m	33.018	33.018	33.018
	L_{to}/m	350.763	354.101	374.609
Six seats		Regular runway ($f=0.025$)	Concrete ground ($f=0.035$)	Hard grass ($f=0.085$)
	L_{tor}/m	288.110	291.557	312.471
	L_2/m	63.565	63.565	63.565
	L_3/m	41.210	41.210	41.210
	L_{to}/m	392.886	396.332	417.246

3. Landing performance calculation

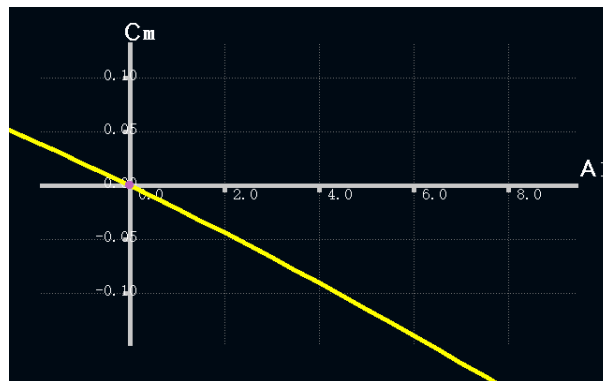
	V_A (m)	L_L (m)
Four seats	38.41	516.17
Six seats	42.34	627.27

5.3 stability analysis

Xflr 5 software is used to analyze the static and dynamic stability of the aircraft

5.3.1 Static stability analysis

The curve of the pitching moment of the whole aircraft with the angle of attack is given. It can be seen that the slope is less than zero, indicating that the aircraft is in a static state, and we have adjusted the installation angle of the horizontal tail to make the aircraft at 0 degree angle of attack (ie, the design in the state of cruise angle of attack). The pitching moment is zero, indicating that the aircraft can fly steadily in this state.



p. 5.3.1 Pitch moment variation curve with angle of attack

We get all kinds of aerodynamic derivatives of the whole machine by analyzing the log files. And then, we get the position of the starting point of the whole machine after the leading edge of the wing 774mm through the analysis of the aerodynamic derivatives. According to our gravity position or the winning first slope, our static stability margin is 0.237, which meets the requirement of longitudinal stability.

We also get the lateral aerodynamic derivatives of the aircraft, and get the rolling stability margin and the yaw stability margin, which are in line with the requirements of the aircraft design manual, as shown in the following figures:

Longitudinal derivatives

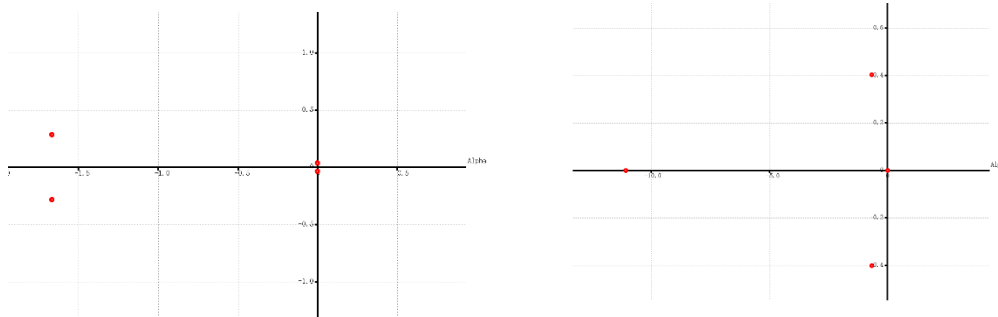
Xu=	-3.5405	Cxu=	-0.0045115
Xw=	145.42	Cxa=	0.1853
Zu=	-417.92	Czu=	-3.1974e-05
Zw=	-4269.8	CLa=	5.4409
Zq=	-4093.7	CLq=	8.3553
Mu=	5.21e-06	Cmu=	5.3168e-09
Mw=	-1179.6	Cma=	-1.2038
Mq=	-12373	Cmq=	-20.225
Neutral Point position=	774.42955mm		

Lateral derivatives

Yv=	-205.81	CYb=	-0.27116
Yp=	-840.65	CYp=	-0.17171
Yr=	1183	CYr=	0.24165
Lv=	-1097.9	Clb=	-0.11213
Lp=	-36015	Clp=	-0.57027
Lr=	4970.4	Clr=	0.078704
Nv=	843.85	Cnb=	0.086184
Np=	-2603.9	Cnp=	-0.041232
Nr=	-5526	Cnr=	-0.0875

5.3.2 dynamic stability analysis

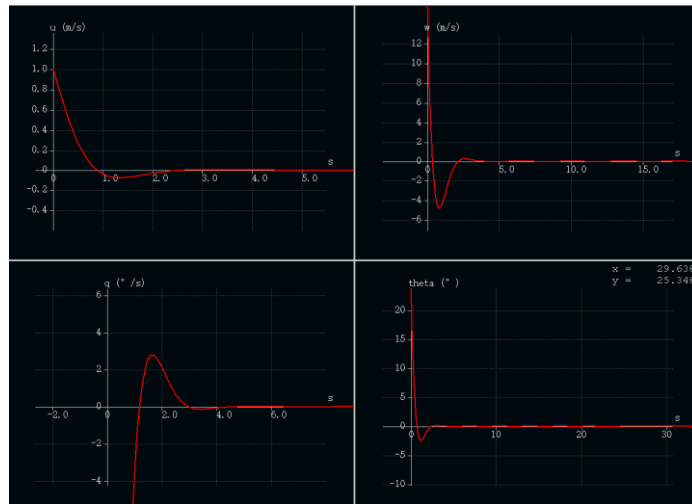
After the static stability analysis, we also analyzed the dynamic stability of the aircraft. According to the distribution of the weight, we calculated the moment of inertia in the xflr5 software, and carried out the dynamic stability simulation analysis in the software, and got the dynamic map after the disturbance, and the aircraft root planting distribution map.



p. 5.3.2 Stability analysis of root distribution

From the longitudinal stability analysis, we can find that the two points on the left are the root distribution of the longitudinal short period movement, and the two points on the right are the longitudinal long period radical distribution. It can be seen from the diagram that the short period is stable and the long period is critical stability, and the short period refers to the fluctuation of the elevation attitude of the aircraft. The long period refers to the fluctuation of flight path when the attitude of aircraft is unchanged. Therefore, the longitudinal stability is in line with the design requirements.

According to the distribution map of lateral stability, the left is the lateral stability, the middle is Holland rolling stability, and the center position is spiral stability. Thus, it can be seen that the stability is in line with the demand.



p. 5.3.3 Curve of longitudinal stability

This is simulation of an aircraft's recovery process after the longitudinal attitude disturbance, and it can be seen from the map that the plane can return to the normal posture in a very short time.

6. Analysis of competitive advantage

6.1 Economic analysis

6.1.1 Cost and usage costs

The total cost of a four-seater aircraft: \$15,125,003.5383

Four-seat aircraft delivery price: \$564,375.5760

The total cost of six aircraft: \$15,893,675.1639

Six aircraft delivery price: \$633046.7062

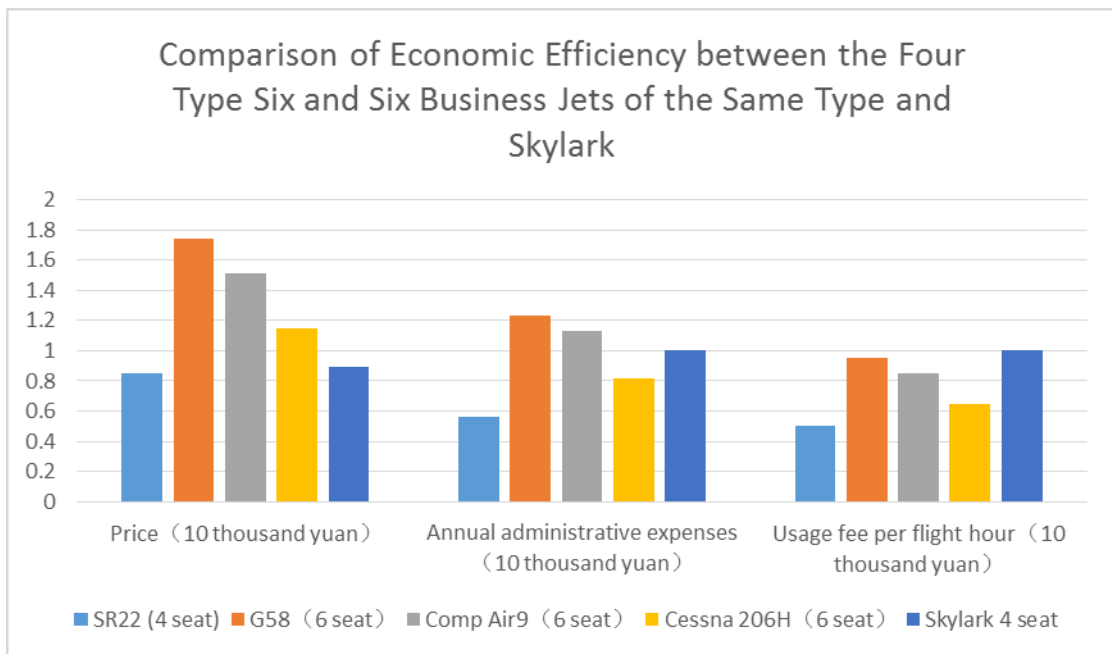
Single flight fuel costs: \$64.1191

Single flight of hydrogen costs: \$70.7670

Total usage fee: \$692.9658

6.1.2 Comparison of the economic performance of the same type of aircraft

	SR22	G58	Comp Air9	Cessna 206H	Skylark 4 seat	Skylark 6 seat
Price (million yuan)	3.42	7.00	6.10	4.61	3.59	4.02.5
Annual administrative expenses (million yuan)	0.31	0.68	0.62	0.45	0.55	0.55
Usage fee per flight hour (thousand yuan)	2.0	3.8	3.4	2.6	4.0	4.0

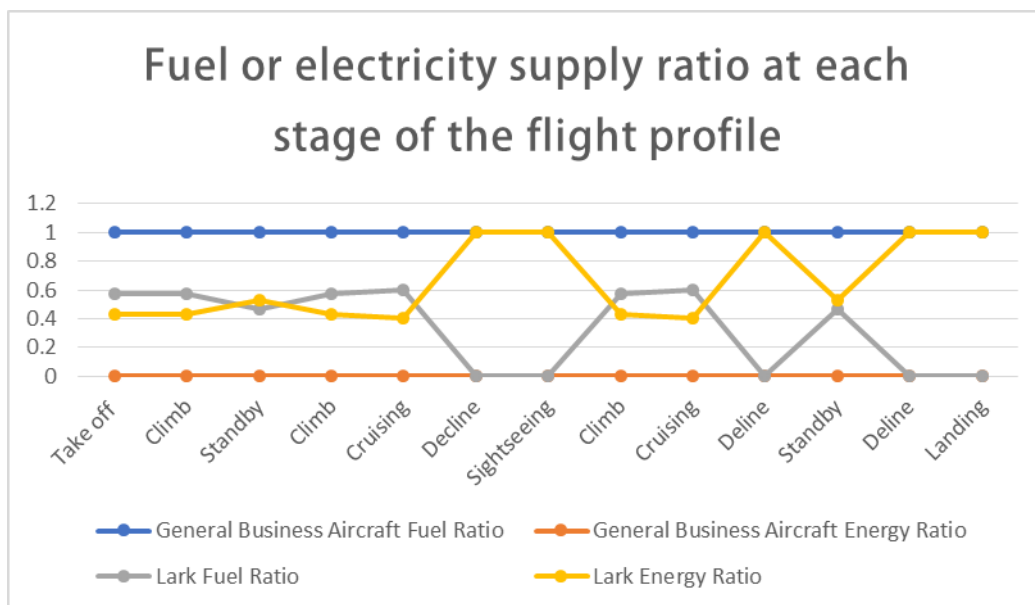


6.2 Environmental protection analysis

6.2.1 Carbon emissions analysis

We use a hydrogen-oxygen fuel cell to power the motor, which has a high specific energy and does not produce harmful gases.

According to calculations, the four-seaters reduced carbon emissions by 70.8% and saved fuel by 140%. Six-seaters reduced carbon emissions by 67% and saved fuel by 100%, which is much higher than the energy-saving average of other hybrid aircraft.



6.3 Competitive Advantage

Compared with other aircrafts of the same type, the Skylark has the following advantages:

(1) The ratio of fuel to electricity can be adjusted to reduce fuel consumption more efficiently.

(2) The noise is small, the light is good, and the cabin environment is relatively comfortable. At the same time, the take-off distance is short. During the takeoff, the total energy consumed is relatively large, and the influence of noise on the outside is greatly reduced.

Comparison of design requirements and final results:

Performance Index	Design Requirements For 4 seats	Our design for 4 seats	Design Requirements for 6 seats	Our design for 6 seats
Maximum flight speed (km/h)	430	456.5	430	453.6
Cruising speed (km/h)	380	392.8	380	466.5
Stall speed (km/s)	80	149.0	80	162.4
Cruising altitude (m)	4900	4900	4800	4800
Theoretical ceiling (m)	5400	11000	5200	11000
Practical ceiling (m)	5300	10800	5100	10500
Range (km)	1900	2005.05	1400	1503.5
Maximum life time (h)	8	5.95	6.5	4.52

Take-off speed (km/h)	115	120.6	125	132.8
Take off rolling distance (m)	340	345.8	430	432.7
Landing speed (km/h)	100	120.6	110	130.1
Landing distance (m)	390	345.8	480	513.27
Climb rate(m/s)	8.0	113.2	7.0	7.97
Payload (kg)	400	422.36	600	602.66

Reference

- [1] Meng Hua, Chuang dodo. Discussion on the side rod technology of cockpit for civil aircraft initiated by Air France AF447 crash [J]. *Jiangsu science and technology information*, 2014 (13): 28-29.
- [2] Wang Huan, Sun Yongrong, Sun Xudong, et al. Research on rod force control method of aircraft active side bar system [J]. *measurement and control technology*, 2016, 35 (12): 79-82.
- [3] B747-400 FCOM, China International Airlines B747 FCOM[S]. Seattle, USA: 2008.10.
- [4] Chen Zhaofeng, Wu Cao, Yang Yong, et al. Study on the preparation of aero grade superfine glass fiber cotton felt and the performance of sound insulation and insulation [J]. *Journal of Nanjing University of Aeronautics & Astronautics*, 2016, 48 (1): 10-15.
- [5] Xiong Du Qin, Guo Xiaozhao, Lu Huiliang, et al. The advantages and disadvantages of aircraft side bar driving device and its improvement design [J]. *human ergonomics*, 2006, 12 (1): 36-38.
- [6] Chen Pu, Xu Hengcheng. Overview of aviation electronic system BIT [J]. *China water transport: Academic Edition*, 2006 (2): 110-112.
- [7] Zhou Yefei, Liu Yantao. Research on partition and resource allocation of integrated modular avionics system for civil aircraft [J]. *civil aircraft design and research*, 2014 (3): 88-91.
- [8] yuan leading double, Liu Meng, Wang Jun. A new environment control system for multi electric aircraft. [C]// large aircraft key technology high level forum and China Aeronautical Society 2007 annual meeting. 2007.
- [9] Hon Man, Deng Zhongwei. Development trend of avionics system for foreign military aircraft [J]. *aviation electronics technology*, 2004, 35 (4): 5-10.
- [10] Han Shumin. High capacity mixed rare earth magnesium nickel based hydrogen storage alloy research [J]. *functional materials information*, 2007 (5): 32.

- [11] Liu Ming. *Foreign aircraft integrated environmental control system [J]. aviation science and technology*, 2004 (2): 28-31.
- [12] Li Xue, Zhang Yi Fang, Qi Weihong, et al. *Progress in [J]. chemistry of nano hydrogen storage alloys*, 2013, 25 (7): 1122-1130.
- [13] Cao Danyan. *Analysis of high altitude adaptability of aircraft cockpit pressure regulating system [J]. technical information*, 2013 (24): 383-383.
- [14] Yuan Xiaojun, Mary. *Development of standards for avionics systems [J]. aviation standardization and quality*, 2002 (6): 8-11.
- [15] Zhang Juncai, Chen Jian. *Design and analysis of Airborne Information System for civil aircraft [J]. technology innovation and application*, 2012 (24): 5-6.
- [16] Zhan Sheng, Du Xiaomei, Jia Hui. *Structural analysis of transmission system of parallel hybrid electric vehicle [J]. light vehicle technology*, 2011 (5): 17-21.
- [17] Liang Yan, Wang Yan, Guo Youyi, et al. *Development status and Prospect of hydrogen storage tanks for hydrogen powered vehicles [J]. cryogenic engineering*, 2001 (5): 31-36.
- [18] AIAA. *Mitigating operational aircraft noise impact by leveraging on automation capability*.
- [19] Wu Wei. *How far is the electric propulsion aircraft from us? [J]. large aircraft*, 2017, (08): 30-33.
- [20] *aviation knowledge [J]. aviation knowledge*, 2007-2017.
- [21] Wu Wei. *How far is the electric propulsion aircraft from us? [J]. large aircraft*, 2017, (08): 30-33.
- [22] Liu Wen. *Multi power source fixed wing UAV power matching and control strategy [D]. Jilin University*, 2017.
- [23] Dong Nianqing. *Current situation, difficulties and Countermeasures of general aviation in China [J]. Journal of Beijing Institute of Technology (SOCIAL SCIENCES)*, 2014,16 (01): 110-117.

- [24] Xiao Zhipeng, Wan Zhiqiang, Liang Meng, Yang Chao. Analysis of aircraft flight loads with two tail braces [J]. *Journal of Beihang University*, 2008, (04): 456-459.
- [25] Wang Libo, Yang Chao, Wu Zhigang. Analysis and optimization of induced drag for aircraft with two tail braces and elastic plane [J]. *Journal of Beihang University*, 2012,38 (07): 867-872.
- [26] Yang Xuan, He Jingwu, Xia Sheng Lai. Aircraft maneuverability analysis of V type tail fin elastic body [J]. *aircraft design*, 2013,33 (02): 13-16.
- [27] Wang Ping. Analysis of the development of business aircraft market [J]. *civil aircraft design and research*, 2013, (02): 5-7+67.
- [28] Li Liang, Sun Qin. Optimization design of T type tail based on Msc.Nastran [J]. *aeronautical computing technology*, 2010,40 (05): 63-66.
- [29] Xu Zhenyu, Lu Qiang. Take-off quality estimation method for fuel cell light aircraft [J]. *aircraft design*, 2011,31 (03): 6-8+23.
- [30] Li Yibo, Lin Peng, Tao Xiaoyang, Hao Xiangdong. Overall parameter design and modeling of air to ground dual fuel cell light aircraft [J]. *aircraft design*, 2016,36 (05): 29-33.
- [41] Li Qingying, daytime, Zhu Chunling. Overview of aircraft mechanical deicing system [J]. *aircraft design*, 2015,35 (04): 73-77.
- [42] Xu Haihua. The rise and fall of the global jet market and China's market outlook [J]. *China civil aviation*, 2009, (12): 65-67.
- [43] Guo Yaobin, Wang Xuejian, Zhang Binjiang. Experimental study on longitudinal aerodynamic characteristics of forward swept wing [J]. *Journal of Aeronautics*, 1987, 6 (6): 227-238. [44] Dongwook Lim, Georgia Institute of Technology; Cedric Justin, Georgia Institute of Technology; Dimitri N. Mavris. Advanced General Aviation Concept Study for a Roadable Aircraft [J]. *15th AIAA Aviation Technology, Integration, and Operations Conference*, 2015, 10.2514/6.2015-3001

[45] Mark D. Moore, NASA Langley Research Center. *Misconceptions of Electric Aircraft and their Emerging Aviation Markets*[J]. *52nd Aerospace Sciences Meeting, 2014, 10.2514/6.2014-0535*

[46] Bryce Roth, Rollin Giffin. *Fuel Cell Hybrid Propulsion Challenges and Opportunities for Commercial Aviation*[J]. *46th AIAA/ASME/SAE/ASEE Joint Propulsion Conference & Exhibit, 2010, 10.2514/6.2010-6537*